THE INFLUENCE OF SITE CONDITIONS AND SURFACE VEGETATION ON SNOW ACCUMULATION AND ABLATION IN THE ELK VALLEY, BRITISH COLUMBIA, CANADA

THE INFLUENCE OF SITE CONDITIONS AND SURFACE VEGETATION ON SNOW ACCUMULATION AND ABLATION IN THE ELK VALLEY, BRITISH COLUMBIA, CANADA

By AARON BEZEAU, B.A., B.Sc.

A Thesis Submitted to the School of Graduate Studies in Partial Fulfillment of the Requirements for the Degree Master of Science

McMaster University MASTER OF SCIENCE (2023) Hamilton, Ontario

TITLE: The Influence of Site Conditions and Surface Vegetation on Snow Accumulation and Ablation in the Elk Valley, British Columbia, Canada

AUTHOR: Aaron Bezeau, B.A. (Mount Royal University), B.Sc. (University of Lethbridge)

SUPERVISOR: Dr. Sean K. Carey

NUMBER OF PAGES: iv, 81

Abstract

Surface mining of coal in the Elk Valley, British Columbia involves the blasting of overburden rock to access the underlying coal formations. Waste rock is placed in adjacent valleys, altering the dynamics of the hydrological process within the watershed. As part of a multi-year R&D program examining the impacts of surface mining on watershed hydrology in the Elk Valley, British Columbia, this study investigates how surface vegetation atop waste rock influences snow accumulation and ablation, and the ability of a physically based model to simulate these hydrological processes. During the 2014 melt season, meteorological observations, eddy covariance turbulent fluxes and snow conditions were measured at three sites; 1) a bare waste-rock surface, 2) a waste-rock surface covered with agronomic grass species, and 3) a mixed pine stand on waste-rock. Variations of meteorological data, turbulent fluxes and measured snow conditions between sites were assessed. Elevation was the dominant control of snow accumulation, with the upper elevation site recording a maximum snow water equivalent of 67 cm, whereas the lower elevation site had a maximum snow water equivalent of 17 cm. Ablation was driven largely by incoming short-wave radiation, which at the bare waste rock and grass covered waste rock sites was greater than the forested site. Turbulent flux contributions to snow ablation were limited in the forested site relative to the bare waste rock and grass covered waste rock sites. The physically based Cold Regions Hydrological Model (CRHM) was able to effectively simulate the influence of vegetated waste-rock surfaces on the hydrological system. However, model parameters regarding vegetation cover and blowing snow required careful calibration to obtain a suitable model output. Results of this study can be used to more accurately model the influence of vegetated waste-rock on the timing and magnitude of the spring freshet in the Elk Valley, British Columbia.

Acknowledgements

The Thesis before you would not have been possible without the guidance and support of the many individuals and organizations.

First and foremost, I would like to thank my supervisor, Dr. Sean Carey for his guidance, support and patience throughout my degree. I also greatly appreciate the opportunity to conduct field research within the Elk Valley, B.C., a place that is second to none.

Second, I would like to thank my field assistants, most notably Nadine Shatilla. Nadine endured an entire winter of fieldwork with me, working long days and late nights. Nadine also provided a sounding board for my thoughts and frustrations during the course of my degree. I would also like to thank my spring field staff: Heather Bonn, Jessica Rastelli and Bernadeta Szmudrowska.

I would also like to thank my technical team. Without the guidance and field support of Dr. Mike Treberg I would never have been able to set up, much less maintain the function of the field instrumentation. And many thanks to Dr. Gord Drewitt and Dr. Victor (Weigang) Tang the MATLAB gurus, for their patience and unwavering willingness to answer my obscure programming questions at all hours of the day, allowing me to keep moving forward.

Thanks as well to the support received from my corporate partners; Rob Klein and Clara Qualizza from Teck Resources limited and Dr. Tyler Birkham and Derek Brown from O'Kane Consulting Limited.

Last, but not least I would like to thank my family and friends for their enduring support.

Table of Contents

List of Figures

List of Tables

1.0 Introduction and Background

Surface mining is a common practice used around the world to access coal deposits. While surface mining is used to mine minerals, metals and oil, it is most often associated with coal, accounting for 40% of coal mined globally and two-thirds of coal production in North America (World Coal Association, 2015). Consequently, surface mining has become the dominant technique for coal mining in North America (Palmer et al., 2010). Mountaintop Mining with Valley Fill (MTM/VF) is the most prevalent surface mining technique for extracting coal in alpine environments, such as those found in the Appalachian and Rocky Mountain ranges (Hendryx et al., 2010; Swanson, 2011; Wayland & Crosley, 2006). MTM/VF is a process by which upper elevation forests are cleared and stripped of topsoil, explosives are then used to break apart rock strata overlying the coal-bearing lithology, and finally, excess rock (mine 'spoil' or 'waste rock') is pushed into the adjacent valleys where it buries existing streams and rivers (Hendryx et al., 2010; Lindberg et al., 2011; Swanson, 2011). Waste rock is typically a heterogeneous mix of overburden material and lower quality coal (Lussier, Veiga, & Baldwin, 2003; Wayland & Crosley, 2006).

Surface mining for metallurgical coal has been ongoing in the Elk Valley, British Columbia, Canada, since 1897, with a rapid increase of production beginning in the 1960's (Lussier et al., 2003). There are currently

five open-pit coalmines (Coal Mountain Operations, Elkview Operations, Line Creek Operations, Greenhills Operation, and Fording River Operations) in this region of southeastern British Columbia, all operated by Teck Resources Limited. Together these mines produce 70% of Canada's total coal exports, making the Elk Valley coal field the most productive in the country (Teck Resources Limited, 2021). The bulk of Teck Resources' coal production comes from the Mist Mountain Formation of the Jurassic-Cretaceous Kootenay Group, while the waste rock consists of overburden, mudstone and siltstone interburden, and coal seams which are too thin or of poor quality (Lussier et al., 2003). These open pit coal mines have an annual coal production volume of approximately 21.9 million metric tons, the majority of which is transported by train to a port near Vancouver, British Columbia, and exported overseas to mainly Asian markets (Teck Resources Limited, 2021). These five open pit mines produce an estimated 140 million metric tons of waste rock each year (Lussier et al., 2003). And by 2010 approximately 4,700 million banked cubic meters of waste rock was stored in the tributaries of the Elk River Valley (Teck Resources Limited, 2014). The Elk River drains a land area of 4,450 km^2 into the trans-boundary of Lake Koocanusa, between Canada and the USA, as part of the Columbia River basin (Figure 1.1).

Figure 1.1: Columbia River Watershed (Wellen et al, 2015)**.**

The MTM/VF process alters the physical landscape and increases the volume and surface area of the geological material available for weathering

and erosion processes, which impacts the hydrological and geochemical fluxes (Dickens, Minear, & Tschantz, 2012; Diehl et al., 2012; Griffith et al., 2012; Lindberg et al., 2011; Wellen et al., 2018). The newly fractured and unconsolidated waste rock is exposed to oxygen and water, accelerating the reaction rates and the release of solutes into the surface water (Swanson, 2011). A considerable amount of water quality research has been conducted on downstream water impacts as a result of surface mining of various minerals, including uranium (Muscatello & Janz, 2009), phosphate (Myers, 2013) and coal (Griffith et al., 2012). Studies of mine affected rivers in Central Appalachian Mountains, USA, as well as, the Elk Valley have reported elevated ion concentrations of chemical constituents of interest (CI) exceeding expected baseline conditions (Chapman, P.M., Berdusco, R.J., Jones, 2007; Griffith et al., 2012; Kennedy, Day, Macgregor, & Pumphrey, 2012; Murphy, Hornberger, & Liddle, 2014; Nordstrom, 2011; Younger, 2004).

In the Elk Valley, considerable attention has been given to increases in concentrations of selenium (Se). Although Se is an essential trace mineral required for growth, development, immune function and metabolism, it can be harmful when it builds up in organic tissue beyond natural levels (Huang et al., 2012; Teck Resources Limited, 2014). Concentrations of Se in Appalachian streams draining surface coal mines almost always exceed locally set management targets for Se concentrations (Palmer et al., 2010). These high concentrations of Se and other chemical CI have shown to have

negative impacts on biodiversity (Pond et al., 2008). High concentrations of Se in fish tissue in the Appalachian region has been documented and has led to the issuance of state advisories against excessive fish consumption by humans (Palmer et al., 2010). Similar to results by Lindberg et al. (2011) who found that the concentration of a number of trace metals, including Se, increased with the proportion of mined area draining to the stream in Appalachia. Documented Se concentrations in the Elk River have increased in association to increases to waste rock volume and are often above British Columbia's aquatic life guidelines (Dessouki & Ryan, 2010; Teck Resources Limited, 2014). While Teck Resources Limited is actively managing concentrations of sulfate, cadmium, nitrate and Se downstream of its mines, nitrate and Se most often exceed local water quality guidelines (Teck Resources Limited, 2014). And Se is the only CI for which water treatment plants have been built (Teck Resources Limited, 2021).

The origin of Se within the Mist Mountain Formation is mainly associated with sulphide, the dominant form of which is pyrite, and the oxidative dissolution of pyrite is likely the origin of selenium leaching into the surface water (Kennedy et al., 2012). Since the 1980's, Se concentrations have been increasing in the Elk River and Se is now part of the regional water quality management strategy (Kennedy et al., 2012). In the late 1990's Teck Coal Limited took steps towards understanding the potential for

environmental effects, mechanisms of selenium leaching and potential attenuation pathways (Kennedy et al., 2012; Teck Resources Limited, 2021).

Research by Wellen et al. (2018) suggests that the export of solutes in mountainous surface mined areas are largely controlled by the transport capacity of the system and not by solubility limitations, at least in the few decades following mining. Therefore, an increase in water movement through waste rock will increase mobilization of weathering solutes such as Se. In practical terms, dry years have less export of solutes than wet years, and sites with unvegetated waste rock release more Se than sites with greater reclamation and vegetation cover, presumably due to increases in net percolation rates (Lindberg et al., 2011; Wellen et al., 2015). This has been further supported in a study by Villeneuve et al. (2017) that reported a reduction in net percolation at adjacent undisturbed areas relative to bare waste rock in the Elk Valley. The primary mechanism for managing near-surface water balances on mined waste rock is through the use of surface covers (Miller & Zégre, 2014; Teck Resources Limited, 2014). However, the practice of salvaging pre-mined soil and organic material, and the placement of this material over waste rock is not widely applied in the Elk Valley. Instead reclamation in the Elk Valley typically involves planting forest vegetation and seeding of agronomic grasses directly atop waste rock. Although the influence of vegetation on the surface water balance has not been directly assessed, research by Wellen et al. (2015) demonstrates that

there is some influence of reclamation on Se loading across a range of water catchments, presumably from reduced percolation. Although reclamation practices have proven to reduce Se concentrations in waterways draining older mines, Se concentrations are significantly elevated in comparison to pre-mine conditions (Lindberg et al., 2011). Minimal research has been conducted on MTM/VF practices in Canada, where hydrological cycles are impacted by cold climates and significantly influenced by the accumulation and ablation of snow.

1.1 Energy Exchange at the Snow Surface

The snow energy balance equation (1.1) is the fundamental physical framework for snowmelt studies (Pomeroy et al., 2007). In a seasonal snowpack, freshly fallen snow is thermodynamically unstable and undergoes a metamorphic process that continues until total melt has occurred (Colbeck, 1982). Numerous mechanisms are responsible for this metamorphic process, and nearly all of these processes result in an increase in density throughout the snow accumulation period (DeWalle & Rango, 2008; Dingman, 2002; Male & Gray, 1981). These metamorphic changes and the melting of the snowpack are caused by vapour density and temperature gradients within the snowpack, which are driven by heat exchange at the snow surface and to a lesser extent at the snow-soil interface (DeWalle &

Rango, 2008; Dingman, 2002; Male & Gray, 1981). The energy balance of a snowpack can be defined as:

$$Q_m = Q^* + SHF + LHF + GHF + Q_R \quad (1.1)$$

Where Q_m is the energy available for melt (W m^{-2}), Q^* is net radiation (W m^{-2}), *SHF* is turbulent flux of sensible heat (W m^{-2}), *LHF* is turbulent flux of latent heat (W m^{-2}), *GHF* is ground heat flux (W m^{-2}), Q_R is the energy due to advection from external sources (W m^{-2}), such as heat added by falling rain and heat derived from patches of soil lying adjacent to patches of snow. This equation is applied to a volume of snow for which the upper boundary is the snow-air interface and the lower boundary is the snow-ground interface (Dingman, 2002). The sign convention for this thesis is that fluxes directed away from the snowpack are negative and those directed towards the snowpack are positive.

Snow accumulation is characterized by its depth and density. These variables are used to calculate the snow water equivalent (SWE) (i.e. the depth of water that would result from the complete melting of the snowpack), which increases during the accumulation period (Male & Gray, 1981). During the accumulation period, the net energy inputs to the snowpack are typically negative and the mean temperature of the snowpack is decreasing (DeWalle & Rango, 2008; Marks, Dozier, & Davis, 1992). The ablation period of a seasonal snowpack begins when the net energy input

becomes more or less continuously positive. The ablation period can be divided into three phases (Dingman, 2002):

i) *Warming*: average snowpack temperatures increase until the snowpack is isothermal at 0°C.

ii) *Ripening*: melting begins to occur but meltwater remains within the snowpack, and once this phase is complete, the snowpack is isothermal at 0°C and cannot retain anymore liquid water.

iii) *Output*: any additional energy inputs result in more melt and meltwater begins to leave the snowpack.

Melt is most often considered to occur at or near the snow surface since this is where the majority of energy available for melt is located. Most studies report that during melt, the radiation fluxes are generally more than latent and sensible heat fluxes, which are larger than ground and advective heat fluxes (DeWalle & Rango, 2008; Dingman, 2002; Male & Gray, 1981).

The snow energy balance equation has been discussed extensively elsewhere in the literature (DeWalle & Rango, 2008; Dingman, 2002; Oke, 1987), therefore a breakdown of individual terms will not be discussed in greater detail in this thesis.

1.2 Mountain Hydrology

In mountain catchments, snowmelt typically makes-up a significant portion of the total annual runoff (Barnett, Adam, & Lettenmaier, 2005; Hock et al., 2006; Pomeroy & Gray, 1995). Snow accumulation and ablation dominate the hydrology of many western Canadian watersheds, and spring freshet results in an annual hydrograph peak, typical of most alpine fed watersheds (Becker, 2005; DeWalle & Rango, 2008; Hoeg, Uhlenbrook, & Leibundgut, 2000; John W. Pomeroy & Gray, 1995). Higher elevations generally accumulate greater SWE (Hardy et al., 2001), as a result of lower air temperatures, higher frequency of snow storms, and reduced evaporation and mid-winter melt events (Herrmann & Bucksch, 2014).

The forested headwaters of these mountain environments help slow the spring snowmelt and assist in the infiltration of surface water into soils at high elevations, thus, playing an important role in the regional hydrologic cycle; partitioning water into fluxes and stores such as snowmelt, transpiration, canopy interception loss and soil moisture storage, which have a direct influence on water use and availability (Chang, 2013; Jonas, Marty, & Magnusson, 2009). Forests that undergo significant changes in the canopy structure as a result of natural or anthropogenic disturbances have subsequent effects on the forest hydrology and snow processes (Helie et al., 2005).

Due to the complex topography and frequent snow redistribution processes in mountain environments, SWE typically exhibits considerable spatial variability even within a given sample location (Bray, 1973; Jonas et al., 2009; Liston & Sturm, 2002). This high spatial variability in alpine environments and forest stand types makes quantifying the watershed scale effects of forest cover change on snowmelt processes difficult. Therefore, accurate modeling of the timing and rate of snowmelt in a post MTM/VF landscape at a single hydrological response unit (HRU) scale provides valuable process information required for modeling the hydrologic cycle of a large forested watershed or a mine scale MTM/VF operation.

1.3 Forest Disturbance Effect on Snow Hydrology

In a forested environment the snow energy balance is highly complex, given the forest canopy's ability to reflect and absorb incoming short-wave radiation, emit long-wave radiation, and alter snow surface albedo (Link & Marks, 1999). The forest canopy also reduces wind speeds by increasing the land surface roughness (Herrmann & Bucksch, 2014). Changes to a forest canopy structure will alter the energy available for snowmelt.

Snow accumulation and ablation processes are well understood in forest versus clearcut (Boon, 2009; Gelfan, Pomeroy, & Kuchment, 2004; Koivusalo & Kokkonen, 2002; Spittlehouse, D.L., Winkler, 1996; Spittlehouse & Winkler,

2005). Removal of the forest canopy due to forest clearing results in an increase of snow accumulation of between 4% to 118% (Golding & Swanson, 1986; Toews & Gluns, 1986). This large variation of snow accumulation in a clearing is partially a result of the size of the forest clearing; small clearings are sheltered by the surrounding forest area, whereas large clearings can lose snow as a result of blowing snow entrainment and redistribution (Pomeroy et al., 2002). Melt rates in a forest canopy can be 30%-300% lower than nearby cleared areas (López-Moreno & Stähli, 2008; Murray & Buttle, 2003; Pomeroy & Granger, 1997; Spittlehouse & Winkler, 2005).

Increased rates of snowmelt in disturbed forests are driven by enhanced snow surface energy inputs as a result of opening the forest canopy (Boon, 2009; Koivusalo & Kokkonen, 2002; Spittlehouse & Winkler, 2005). In cleared forests, Q* is driven by incoming short-wave radiation (K↓) because removal of the forest canopy removes the forest's ability to attenuate K↓ (Ni et al., 1997). Removal of the forest canopy decreases the amount of downward long-wave radiation (L↓) emitted from the canopy. Removal of the forest canopy may result in negative values of net long-wave radiation (L*), due to the fact that upward long-wave radiation (L↑) from the snow surface is not compensated by L↓ from the forest canopy (Boon, 2009). The removal of the forest canopy will decrease the land surface roughness and increase wind speeds, which will subsequently enhance turbulent heat fluxes (Boon, 2009; Koivusalo & Kokkonen, 2002).

Snow interception by the forest canopy is a crucial factor driving the spatial distribution of the sub-canopy snowpack (Hedstrom & Pomeroy, 1998). Snowfall interception by branches and needles of trees can be stored; sublimated back into the atmosphere; resuspended and redistributed by high winds; or unloaded as accumulated snow and meltwater to the ground surface (Pomeroy & Goodison, 1997) (Figure 1.2). The most common cause of snow loss in a forest environment is from sublimation of the canopy snow load (Pomeroy & Schmidt, 1993; Schmidt, Jairell, & Pomeroy, 1988; Winkler & Boon, 2014), accounting for up to 45% of annual snowfall loss in Western Canada (Pomeroy, Gray, & Shook, 1998).

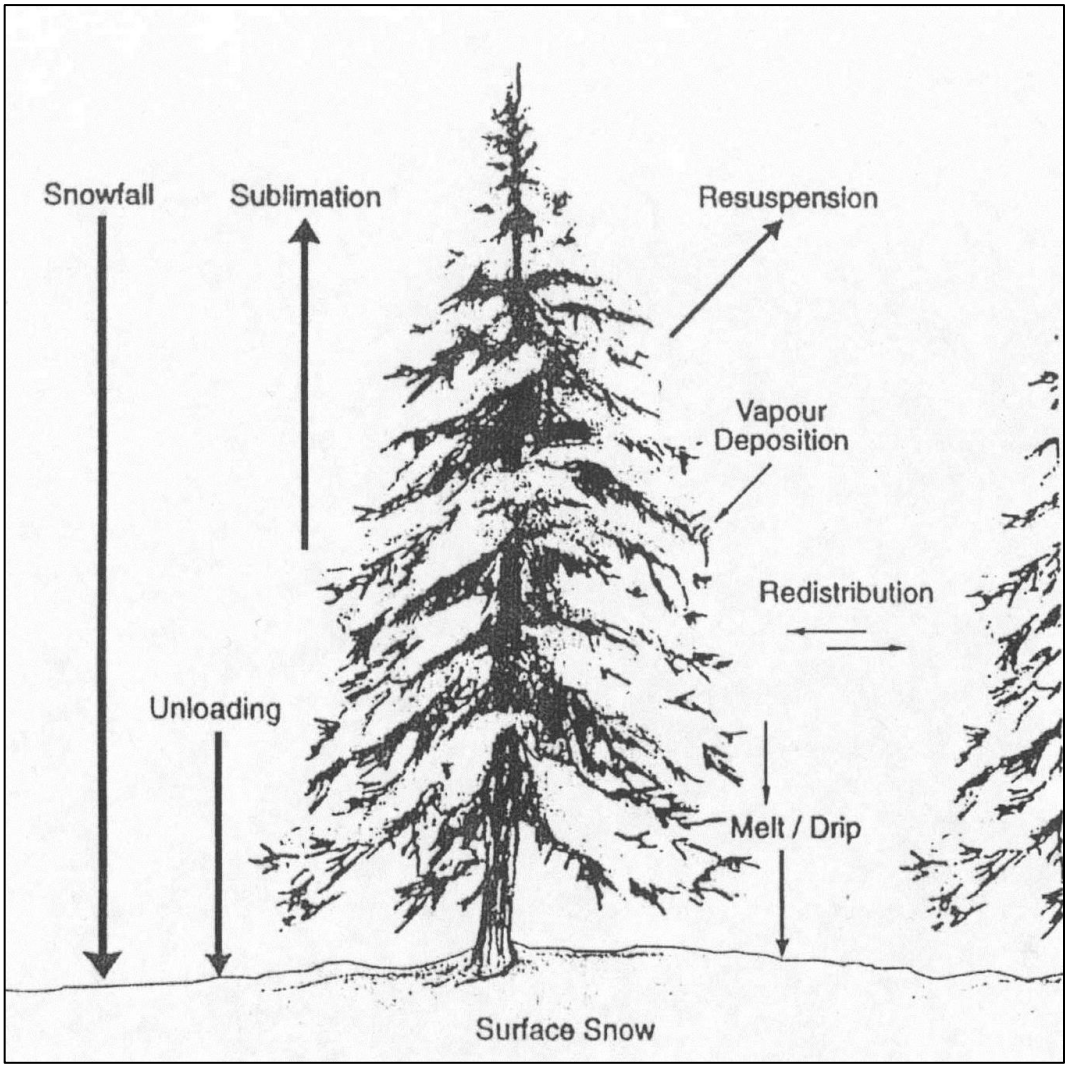

Figure 1.2: Disposition of winter snowfall in a boreal forest (Pomeroy & Schmidt, 1993)**.**

1.4 Numerical Snow Models

The major variables, which characterize a snow cover are; SWE, snowpack depth, vertical density and temperature profiles, liquid water content, and albedo. Numerous snowmelt models have been created to simulate the evolution of some or all of these variables, and range in their

complexity, from; i) simple index methods like The Snowmelt Runoff Model (SRM) (Martinec, Rango, & Major, 1983), ii) energy budget methods like The Snowcover Energy and Mass-Balance Model (SNOBAL) (Marks & Dozier, 1992), iii) full solutions of the equations of flow of energy and mass like the Simultaneous Heat and Water Model (SHAW) (Flerchinger, 2000). Regardless of the model's complexity, the conservation of energy is the fundamental foundation of all snowmelt models (Gray & Landine, 1987). To model turbulent fluxes, some models rely on empirical relations for SHF and LHF (Gray & Landine, 1988). However, more recent models tend to utilize some variation of the bulk transfer method (e.g. SNOBAL).

Rutter et al. (2009) compared 33 snowpack models of varying complexity at five locations in the Northern Hemisphere for up to two winter seasons, across a range of hydrometeorological and forest canopy conditions. Modeled estimates of depth or SWE were compared to observations at open and forested sites. Results showed that SWE was easier to model at open sites than forested sites. Rutter et al. (2009) concluded there was no universal "best" model for all locations, and a model that performed well at an open site was unlikely to perform well at a forested site and vice versa.

1.5 State of the Science

Despite concerns due to rising Se concentrations in the Elk Valley, there is a limited understanding of Se release and mobilization from waste rock, and how surface mining and reclamation practices alter the hydrological processes at a basin scale (Jayaweera & Biggar, 1996; Miller & Zégre, 2014; Murphy et al., 2014; Nicholls, Drewitt, Fraser, & Carey, 2019; Shatilla, 2013; SRK Consulting Ltd., 2010; Swanson, 2011; Wellen et al., 2015, 2018). In 2012 Teck Resources Limited initiated a multi-disciplinary research and development program to investigate the influence of surface coal mining and the subsequent fate and transports of CI from waste rock dumps in the Elk Valley. Previous work in the Elk Valley and the USA has typically focused on the enrichment of Se in ground water (Bailey, Gates, & Halvorson, 2013; Hanna & Loftis, 2007; Myers, 2013; Shatilla, 2013; Villeneuve, Barbour, Hendry, & Carey, 2017; Wellen et al., 2018), and no research to the author's knowledge has specifically studied the impact of reclamation on snow accumulation and ablation processes and how reclamation could impact the transport capacity of Se in a waste rock dump. Research by Wellen (2015) found that basin-wide export of Se in the Elk Valley "is greater in wet years than dry years and that waste rock with vegetative cover releases less Se than bare waste rock". Wellen's (2018) results further alluded to the importance of better understanding the impact of reclamation on the local hydrology and the subsequent impacts of Se loading by suggesting the

release of Se is limited by transport capacity rather than Se availability. Minimal knowledge exists on how Se loading changes as a result of factors that can be controlled during or after the mining process, such as the presence or type of reclamation. This gap in knowledge makes it difficult to recommend science-based approaches to managing Se in MTM/VF operations and to forecast Se concentrations and loading associated with future use development. The purpose of this study is to help fill in the gaps of knowledge associated with reclamation practices and Se loading on a MTM/VF waste rock dump.

1.6 Objectives

The specific objectives of this study are to 1) identify how site conditions and surface vegetation atop waste rock influence snow accumulation and ablation, 2) determine if processes of snow accumulation and ablation can be simulated using a physical based model and 3) determine if a physical based model can be used to model forest reclamation scenario testing. No previous research has incorporated the potential impacts that reclamation practices could have on snow accumulation and ablation in a MTM/VF landscape and the subsequent effects reclamation could have on net percolation. This research helps to address knowledge gaps that exist in the relationship between hydrology and geochemistry in a mountainous surface mined

system, which interact to determine the quantity of CI that are transported to streams.

1.7 Thesis Structure

This thesis is divided into 5 chapters. Chapter 2, **Methods**, follows chapter 1, **Introduction and Background**. Chapter 2 provides a detailed description of the research location, the specific study sites, as well as, an overview of the methods used to gather field data and how the data was analyzed. Chapter 3, **Results,** provides the outcomes of the data acquired in the previous chapter. Chapter 4, **Discussion**, provides a detailed treatment of the results and the implications of these results. The 5th and final chapter, **Conclusion**, summarizes the key findings of this research and provides insight into the potential next steps of this research.

2.0 Methods

2.1 Site Description

Research for this thesis was conducted in the Elk Valley, British Columbia, Canada from March 24 to June 19, 2014. The Elk Valley is located in the southeast corner of British Columbia, within the Kootenay region on the west side of the Rocky Mountains (Figure 2.1).

For this study, three waste rock sites were chosen: a reclaimed forest site, an agronomic grass site, and a bare waste rock site. The forest site was located at Teck Coal's Fording River Operations Mine, while the grass and bare waste rock sites were located on Teck Coal's Line Creek Operation Mine. Fording River Operations is located 30 km north of Line Creek Operations, while the agronomic grass and bare waste rock sites are located 300 m apart at Line Creek Operations Mine.

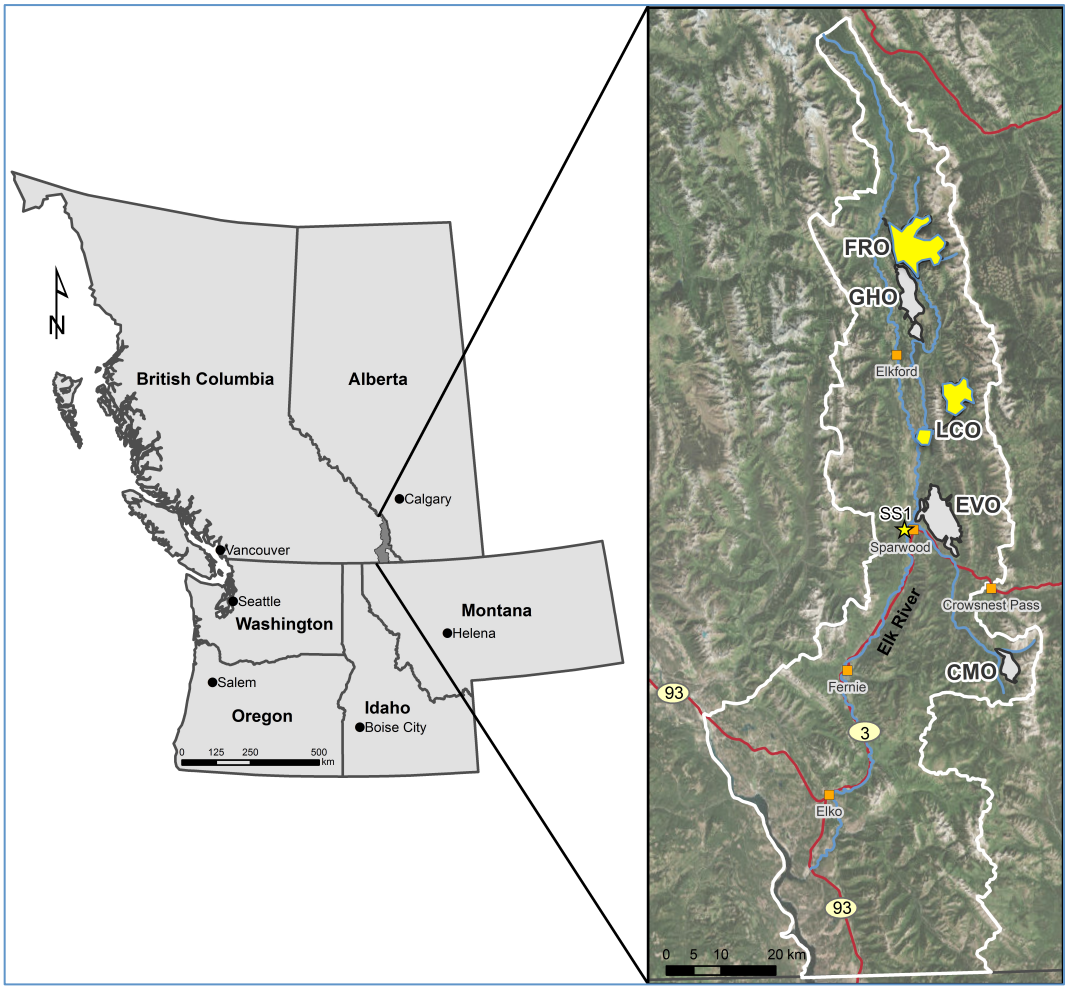

Figure 2.1: Location map of the Elk River Valley, British Columbia, Canada, and regional coal mining operations (FRO, GHO, LCO, EVO, CMO). FRO mine was the study site for the reclaimed forest, LCO mine was the study site for the reclaimed grass site and the bare waste-rock site (highlighted in yellow). The limits of the Elk River watershed boundary are delineated with a solid white line; the watercourses and lakes are indicated in blue; red lines and numbers in yellow ovals indicate highways (Villeneuve et al., 2017).

2.1.1 Climate

The climate of the region is characterized as humid continental, with a mean annual temperature of 4.4°C and a mean annual precipitation of 613 mm. Mean winter temperatures range from -2°C to -7°C and summer mean temperatures range from 9°C to 15°C. Winter and summer extreme temperatures range from -38°C to 36°C, respectively. Precipitation predominantly comes as frontal systems; however, convective storms are common during late summer. Climate norms for the area show that 30% of annual precipitation falls as snow, with 411 mm as mean rainfall and 264 cm as mean snowfall. Climate Normals were provided by Environment Canada, Sparwood weather station (1981-2010, 1,138 m a.s.l., ID: 1157630) (Environment Canada, 2021). Precipitation and temperature within this alpine environment are highly variable due to microclimatic factors and are therefore difficult to accurately measure on a larger scale (Marks et al., 1992). Topographic relief and the region's annual temperature and precipitation lapse rates are approximately −0.48 °C/100 m and +21 mm/100 m (Barbour, Hendry, & Carey, 2016), which significantly impacts the proportion of precipitation that falls as snow. Records from 2012 suggest that between 1300 m and 1850 m elevations, the portion of snow to rain varied from 28% to 66%, respectively (Shatilla, 2013).

2.2 Study Sites

2.2.1 Reclaimed Forest Site

This site is located on a 26°, east aspect slope, at an elevation of 1700 m a.s.l. (50° 09.848' N, 114° 52.711' W). This site is characterized by a reclaimed forest stand (Figure 2.2a) that was planted as test plots in the 1980's. These test plots are loosely organized in 25 m by 25 m grids, consisting of both uniform and mixed Lodgepole Pine (*Pinus contorta*) and Engelmann spruce (*Picea engelmannii*) stands (IEG Consultants Ltd., 2013). Due to the harshness of the waste rock substrate, tree spacing and growth is non-uniform. The forest has a mean tree height of 6.16 ± 0.09 m and a mean stand diameter of 6.23 ± 0.15 cm (IEG Consultants Ltd., 2013). The average leaf area index (LAI) of the site is 2.79 ± 1.19 m^2 m^{-2} (IEG Consultants Ltd., 2013). The understory vegetation consists of bird's-foot trefoil (*Lotus corniculatus*), Screw Moss (*Tortula sp*.), Thread Moss (*Bryum sp*.), Golden Ragged Moss (*Brachythecium salebrosum*), Redtop (*Agrostis gigantean*), Great Mullein (*Verbascum Thapsus*) and assorted grass species (Nicholls et al., 2019). The waste rock surface has no soil cover, and the top 1 m of waste rock substrate on which the vegetation has grown is comprised of 74% coarse gravel and cobble, 19% sand, and 7% silt and clay (O'Kane Consultants Ltd., 2013).

2.2.2 Agronomic Grass Site

This site is located on a 13°, south aspect slope, at an elevation of 2076 m a.s.l. (49° 56.782' N, 114° 47.747' W). This site is characterized by agronomic grasses and legumes (Figure 2.2b), including alfalfa (*Meducago sativa*), hard fescue (*Festuca trachyphylla*), thickspike wildrye (*Elymus lanceolatus*) and red fescue (*Festuca rubra*) (Nicholls et al., 2019). The average LAI of this site is 1.82 ± 0.79 m^2 m^{-2} (IEG Consultants Ltd., 2013). The top 1 m of waste rock substrate consists of 54.7% coarse gravel and cobble, 38.9% sand, and 6.4% silt and clay (O'Kane Consultants Ltd., 2013).

2.2.1 Bare Waste Rock Site

This site is located on flat terrain (<5° slope), at an elevation of 2146 m a.s.l. (49° 56.941' N, 114° 47.682' W). This site is characterized by exposed bare waste rock (Figure 2.2c). Seedlings were planted, however, no vegetation germinated. The top 1m of waste rock substrate consists of 77% coarse gravel and cobble, 18% sand, and 5% silt and clay (O'Kane Consultants Ltd., 2013).

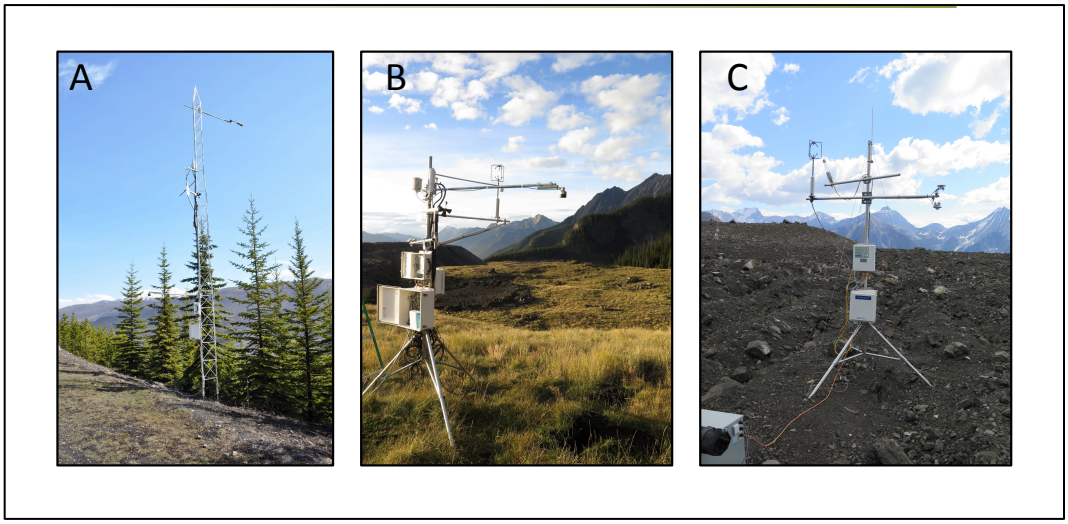

Figure 2.2: Study sites; (a) Reclaimed Forest, (b) Agronomic Grass, (c) Bare Waste Rock. Photos taken in Sept 2013.

2.3 Field Methods

2.3.1 Snow Surveys

Peak snow accumulation and snowpack ablation were measured as snow water equivalent (SWE) during the 2014 snow season using a combination of snow pits and snow courses; measuring depth and density, using a snow probe and snow tube, respectively (Figure 2.3). Manual snow depth measurements were compared to continual snow measurements using a SR50A sonic distance sensor (Campbell Scientific Ltd.) recording on 15-minute time intervals.

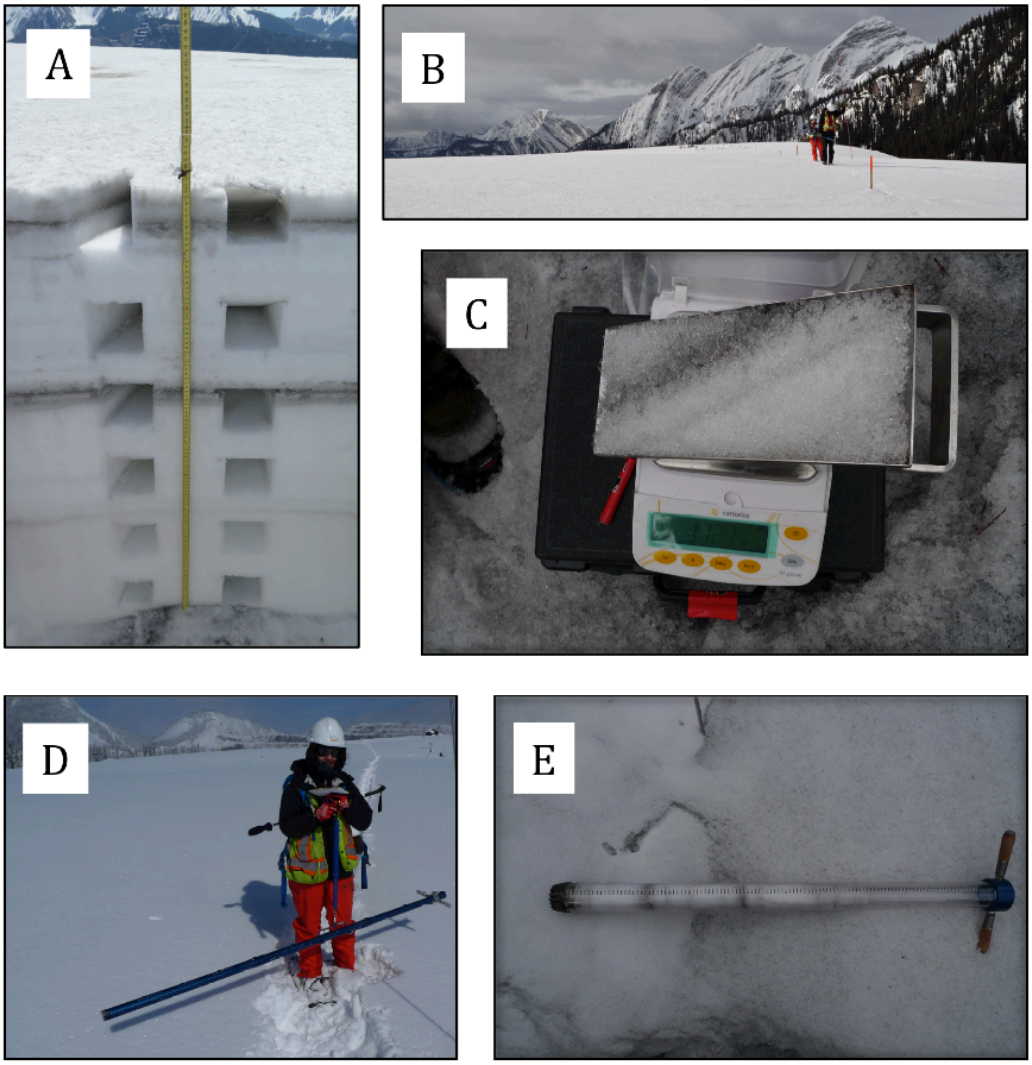

Figure 2.3: Snow survey methods; (a) Snow pit, (b) snow transect, (c) snow density measurement with a 250 cc density cutter, (d) Snow density along transects measured with the Federal snow tube, (e) Snow-Hydro snow tube.

Snow survey transect locations and length were determined based on terrain features of slope and aspect, as well as, vegetation type and density (Figure 2.4), with the goal of accurately representing the HRU of each study site (Watson et al., 2006; Woo, 1997). Transect lengths ranged from 50 m to

60 m at the reclaimed forest site due to the overall smaller size of this study site and due to the size of the reclaimed vegetation sample plots. Transects at the agronomic grass site and the bare waste rock site were 50 m to 200 m, as the terrain was more uniform at these sites and the HRU's of these sites were larger compared to the reclaimed forest site. Transects were staked at 0 m and at 25 m increments for the length of each transect. Snow courses were "permanently" marked with stakes (Figure 2.3b) to ensure that subsequent sampling occurred in a well-defined area to limit the effects of confounding factors such as vegetation cover and topography (Dixon & Boon, 2012; Male & Gray, 1981; Woo, 1997).

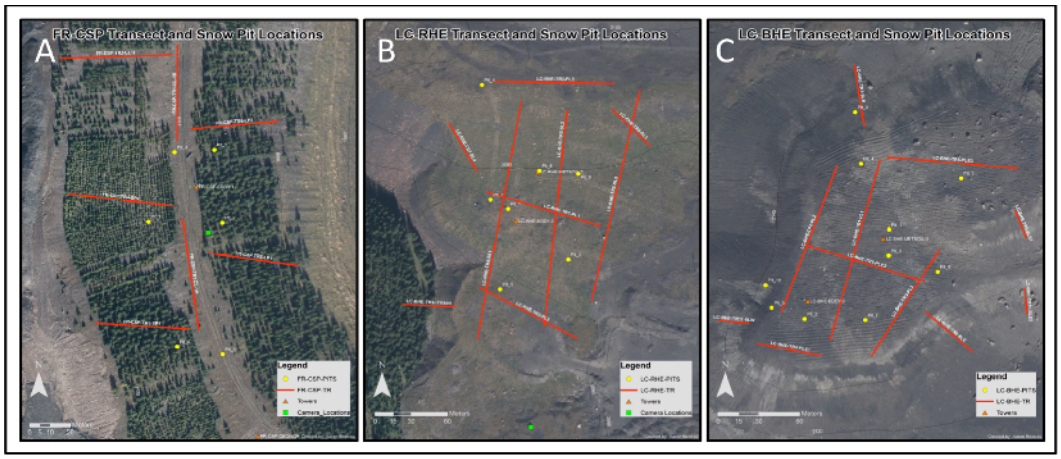

Figure 2.4: Transect and snow pit locations; (a) Reclaimed Forest, (b) Agronomic Grass, (c) Bare Waste Rock. Red lines delineate transects, yellow circles show snow pit locations.

Previous studies have determined that density measurements of $n \geq 30$ give a power of approximately 0.9 to detect at least 30% difference in peak

SWE between sites (p=0.05) (Spittlehouse, D.L., Winkler, 1996). Woo (1997), states that for transects of 100 m, there should be 20 to 40 depth measurements and 1 or 2 density samples. To ensure this level of statistical significance (or greater), depth measurements were taken every 5 m and snow tube density measurements were taken at 0 m and every 25 m. This protocol resulted in snow depth measurements of n=81, n=140 and n= 142, and snow density measurements of n=31, n=32 and n=34 for the reclaimed forest site, the agronomic grass site and the bare waste rock site, respectively. Snow surveys began the first week of April, prior to peak SWE, and weather permitting were conducted weekly at each site until the snowpack was gone. Average snow depth (cm) and density (g cm^{-2}) were multiplied to calculate SWE for each site.

Snow density was measured with either the Snow-Hydro (Snow-Hydro, Fairbanks, Alaska, USA) or the Federal (GeoScientific Ltd., Vancouver, British Columbia, Canada) snow tubes. Both snow tubes are equipped with a cutting head allowing the snow tubes to cut through any ice lenses or consolidated snow layers within the snowpack and into the ground surface to obtain a dirt plug to ensure accurate samples. The dirt plug was removed prior to weighing and the snow core was re-sampled if a dirt plug was not present.

Sampling with the Federal snow tube (Figure 2.3d) was required at the agronomic grass and bare waste rock sites for the majority of the sampling period due to the depth of the snowpack (>140 cm). Sampling at the

reclaimed forest site was exclusively done with the Snow-Hydro snow tube (Figure 2.3e) as the snowpack was consistently shallower than the other sites and the snowpack was more heterogeneous due to more significant diurnal freeze/thaw cycles at the lower elevation. As the snowpack decreased at the agronomic grass and bare waste rock sites and the snowpack became increasing isothermic, more sampling was done at these sites with the Snow-Hydro snow tube as the larger radius (3.09 cm) was more effective in sampling an increasingly ripened snowpack than the Federal snow tube (2.07 cm radius). These observations were consistent with findings by (Dixon & Boon, 2012). For the purpose of this study, snow tube types were seen as interchangeable as previous studies show minimal differences (<10%) in measured SWE between the two snow tubes (Dixon & Boon, 2012; Lillquist & Walker, 2006).

Snow pits were dug on a weekly basis (weather permitted) during the snow sampling period in order to acquire a more detailed snow profile than was provided by the snow courses and as a means to calibrate snow course measurements (Figure 2.3a). Snow temperature and density were measured at 10 cm intervals using a digital thermometer (SnowMetrics, Fort Collins, Colorado, USA) and a 250 cc density cutter (Figure 2.3c) (SnowMetrics, Fort Collins, Colorado, USA), respectively.

2.3.2 Continuous Measurements

Each of the three study sites was instrumented with a meteorological tower (Figure 2.2). Meteorological towers recorded wind speed and direction (R.M. Young Model 05103AP-10 Wind Monitor), air temperature and relative humidity (HMP45-HC2-S3 probe), net radiation (CNR4 Kipp and Zonen at the forest and grass sites; NR-LITE2-Kipp and Zonen at the bare waste rock site), snow depth (SR50A) and soil temperature at 0.05 m and 0.1 m below the surface at the reclaimed forest and agronomic grass sites (107-L Campbell Scientific) (Table 2.1; Table 2.2). Shielded total weighing precipitation gauges (Geonor T200B) measured precipitation for each site.

To measure latent and sensible heat fluxes using the eddy covariance method, each tower was instrumented with a three-axis sonic anemometer (R3-50, Gill Instruments Ltd.) and an infrared gas analyzer (IRGA). A closed path LICOR-7200 was installed at the reclaimed forest and agronomic grass sites and an open-path LICOR-7500 was installed at the bare waste rock site. Eddy covariance instrumentation heights were 5.2 m, 3.0 m and 3.4 m at the reclaimed forest, agronomic grass and bare waste rock sites, respectively. Due to the slope of the land and the location of the meteorological tower at the reclaimed forest site, the eddy covariance instrumentation was above the tree canopy despite the recorded height differential between the canopy and tower height.

		Instrumentation height (m)		
Variable	Instrumentation	Reclaimed Forest	Agronomic Grass	Bare Waste Rock
Temp, RH	HMP45	2	2	2
Precip	Geonor	1	1	1
Wind Speed, direction	R3-50 3D soncic anemometer-thermometer / RM Young 05103 Wind Monitor	5	2	2
Turbulant Fluxes	LiCOR Li-7700	5.2	3	3.4
Net Radiation	CNR4	9	1.5	
Net Radiation	NR Lite 2			2
Snow Depth	SR50A	2	2	2
Soil Temp	Heat Flux Plate	0.05	0.05	0.05

Table 2.1: Instrumentation and measurement height at each research site.

Research site	Instrumentation	Elevation (m a.s.l.)
Reclaimed Forest	Geonor	1699
Reclaimed Forest	Met	1700
Agronomic Grass / Bare Waste Rock	Geonor	1811
Agronomic Grass / Bare Waste Rock	Soil-Met	1797
Agronomic Grass	Met	2073
Bare Waste Rock	Met	2147

Table 2.2: Instrumentation elevation at each research site.

2.4 Data Analysis

All meteorological variables were scanned at a frequency of 10 Hz and recorded on a Campbell Scientific data-logger at 30-minute time intervals. Latent and sensible 30-minute fluxes were computed from high frequency

signals with EddyPro version 6.1 using blocking averaging, planer fit coordinate rotation and WindMaster Pro wind velocity correction multipliers (Wilczak, J.M., Oncley, S.P. & Stage, 2001). To compensate for open-path IRGA gas concentration density fluctuations the Webb Pearman Leuning (1980) correction was applied. Densities of H_2O and CO_2 were direct outputs by the closed-path IRGA therefore no correction was applied. Time lags were detected and compensated through covariance maximization. Spike detection and removal were computed according to Vickers and Mahrt (1997). For all sites the Moncrieff, Clement, Finnigan and Meyers (2004) analytic correction for high-pass filtering was computed. Correction for low-pass filtering effects were evaluated for the open-path and close-path systems using methods by Moncrieff et al. (1997) and Horst (1997), respectfully. When turbulence was insufficient (friction velocity <0.1 m/s) fluxes were removed. Short gaps in data were filled using the mean diurnal variation method, replacing missing values with the mean for that time period over the previous and subsequent 7-day period (Falge, Baldocchi, & Olson, 2001). Latent and sensible heat fluxes were filled using artificial neural networks created in MATLAB (Mathworks Inc., Massachusetts, USA) neural network tool-box (Nicholls et al., 2019). Latent heat was modeled with net radiation, air temperature, binary nighttime vector and relative humidity. Sensible heat was modeled using the same parameters used to gap-fill latent heat fluxes.

2.4.1 Snow Energy Balance

Differences in snowmelt energy balance characteristics between the reclaimed forest, agronomic grass and bare waste rock sites were calculated and compared using the snow energy balance equation (1.1). Most variables in the snow energy balance equation were measured directly at each site, however, some clarification is required for variables Q*, SHF, GHF, Q_R, Q_{cc} (cold content of the snowpack) and T_s (mean snowpack temperature).

The NR Lite 2 net radiometer located at the bare waste rock site only measured Q* and does not provide output values for net short-wave radiation (K*) or L*, therefore comparisons of radiative fluxes between all three sites was limited to Q*.

Discontinuous measurements of SHF was due to power constraints as a result of prolonged periods of snowfall preventing access to site and the ability to clear the solar panels of snow.

The bare waste rock site was not equipped with heat flux plates. Due to this site's 300 m proximity and 70 m difference in elevation compared to the agronomic grass site, the difference between these sites with regards to GHF was estimated to be negligible, and previous research has documented the minimal effects of GHF on model performance due to the small contribution of GHF to total energy (Ellis, Pomeroy, Brown, & MacDonald, 2010; Link & Marks, 1999). Therefore, the GHF value for the bare waste rock site was

calculated using the GHF values from the agronomic grass site plus the region's temperature lapse rate of −0.48 °C/100 m (Barbour et al., 2016).

One rain-on-snow event (ROS) was observed at the agronomic grass and bare waste rock sites on April 11 totaling < 4 mm at each site, and the ROS events that occurred at the reclaimed forest site late in the ablation season did not cause rapid snow surface melting in the continuous snow depth record from the SR50A. Therefore, advective energy from ROS was not considered in this model.

Internal snowpack processes are also not physically represented due to a lack of measured data during the melt period. Therefore, they are empirically incorporated by calculating average T_s as a function of the previous three days' air temperature (USACE, 1998), and setting melt to zero at all sites during periods when T_s < 0 °C. This requires that T_s return to 0 °C following cold periods prior to melt re-initiation.

2.4.2 Cold Regions Hydrological Model (CRHM)

The Cold Regions Hydrological Model (CRHM) has been discussed extensively (Ellis et al., 2010; Pomeroy et al., 2007; Pomeroy, Fang, & Ellis, 2012), so only a brief overview is presented here. CRHM is a physically based empirical model, built on a system of interdependent modules that permits appropriate hydrological processes for the basin, selected from a

library of process modules, to be linked to simulate the hydrological cycle of HRUs (Pomeroy et al., 2007) (Figure 2.5).

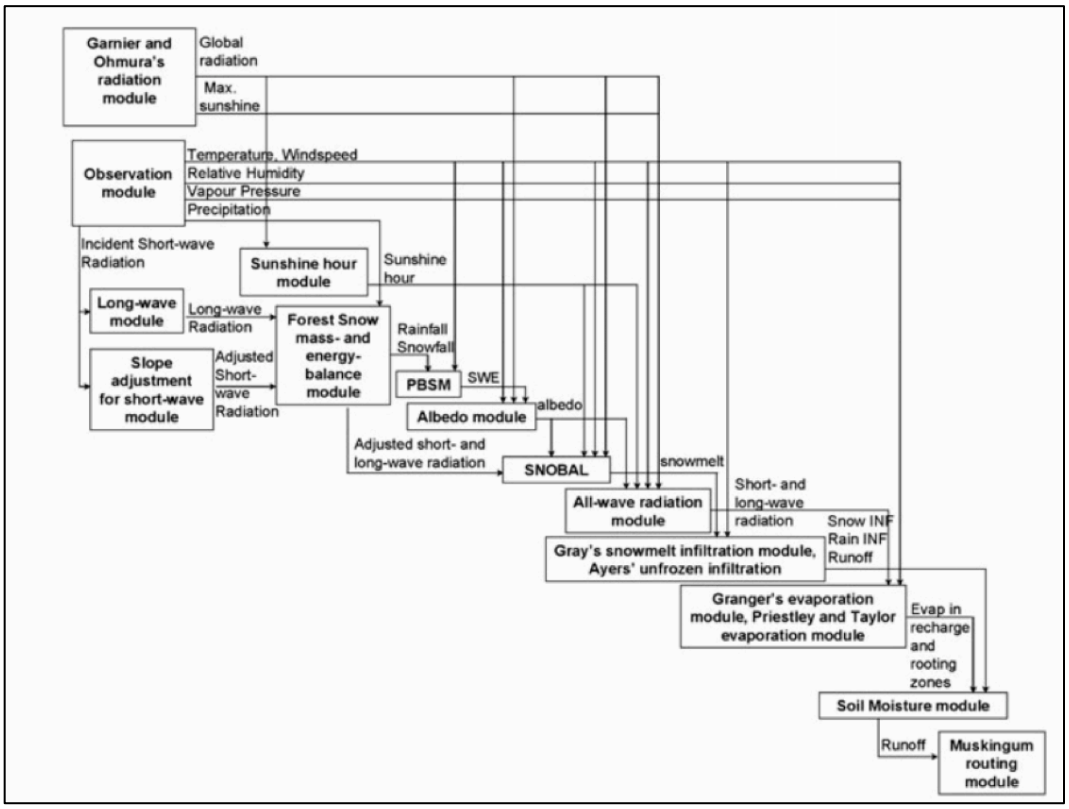

Figure 2.5: Cold Region Hydrological Model (CRHM) Interaction of state variables and fluxes calculated by cascading modules. (Pomeroy et al., 2007)

CRHM operates through interaction of its four main components (Ellis et al., 2010):

i) *Observations*: CRHM requires the following meteorological forcing data for each simulation time step:

   a. air temperature, T_a (°C);

b. humidity, either as vapour pressure, e_a (KPa) or relative humidity, RH (%);
c. precipitation, P (kg m^{-2});
d. wind speed, observed either above, or within the canopy, u (m s^{-1});
e. shortwave irradiance, K↓ (W m^{-2}) (in the absence of observations, K↓ may be estimated from T_a);
f. longwave irradiance, L↓ (W m^{-2}) (in the absence of observations, L↓ may be estimated from T_a and e_a);

ii) *Parameters*: provides a physical description of the site, including latitude, slope and aspect, forest cover density, height, species, and soil properties. In CRHM, forest cover need only be quantified by an effective leaf area index (LAI) and forest height (h); the forest sky view factor (v) may be specified explicitly or estimated from LAI. The heights at which meteorological forcing data observations are collected are also specified here.

iii) *Modules*: algorithms implementing the particular hydrological processes are selected here by the user.

iv) *Initial states and variables*: specified within the appropriate module.

The module output used for this study was SNOBALCRHM, an adaptation of the physically based two-layer snow energy and mass balance model first

introduced by Marks & Dozier (1992), and described in detail by Marks et al. (1998). SNOBAL calculates the energy balance of the snow cover using equation (1.1) and is driven by the six forcing variables detailed in section i) *Observations*. For the purpose of this study the model was run with one HRU for each site.

SNOBALCRHM was chosen for this research project for three main reasons; First, the model's origin and validation sites are located in the Marmot Basin (Pomeroy et al., 2012), a similar mountain environment less than 150 km north of the Elk Valley. Second, CRHM has been widely used and has shown promising results in alpine environments (DeBeer & Pomeroy, 2010; Ellis, Pomeroy, & Link, 2013; Pomeroy et al., 2012; Pomeroy & Granger, 2005). Finally, SNOBALCRHM requires modest data and parameter requirements for model output.

2.4.3 Model Performance

Model performance was evaluated by comparing the timing of observed versus modelled snowpack removal. Performance was also assessed by comparing continuous records of observed SWE (SR50A snow depth and field snow density measurements) and modelled SWE for each of the three sites. The regression coefficient was used as a measure of goodness-of-fit between observed and modeled SWE. Internal model function was also evaluated by calculating the regression coefficient, mean absolute error

(MAE), and total error between observed and modeled snow energy balance variables.

3.0 Results

3.1 Climate

The year 2014 was an average snow year, with an annual snowpack 98% of the 30-year normal (Environment Canada, 2021). The mean air temperature at the Environment Canada Sparwood weather station (ID: 1157630) from April 1 to June 1 was 7 °C, matching the 30-year climate normal of 7 °C. Mean daily air temperature was warmer at the low elevation reclaimed forest site, whereas temperatures were only slightly warmer at the agronomic grass site compared with the bare waste rock site. From April 1 to June 1, mean air temperatures at the reclaimed forest, agronomic grass, and bare waste rock sites were 3.7, 0.9, and 0.7°C, respectively (Table 3.1; Figure 3.1). The higher temperature at the reclaimed forest site was attributed to the valley's adiabatic lapse rate. Variability in relative humidity (RH) between the three sites was minimal. Mean wind velocity at the reclaimed forest, agronomic grass and bare waste rock sites was 1.2, 1.9 and 2.7 m $s^{-}1$, respectively.

Snowfall occurred almost daily at each site until being observed as snow free (Figure 3.1). The last recorded significant snowfall (> 5 cm) at the reclaimed forest site occurred on May 3, for a total snow input of 8.3 cm, and the last recorded snowfall input for this site was May 5, for a total snow input of 2.9 cm. In May and June the agronomic and bare waste rock sites recorded minimal (< 5 cm) daily snow inputs until becoming snow free. In May, the

agronomic grass and bare waste rock sites had two significant snow inputs; on May 5th, they received 16 cm and 19.6 cm, and on May 9th, they received 7.9 cm and 8.5 cm, respectively.

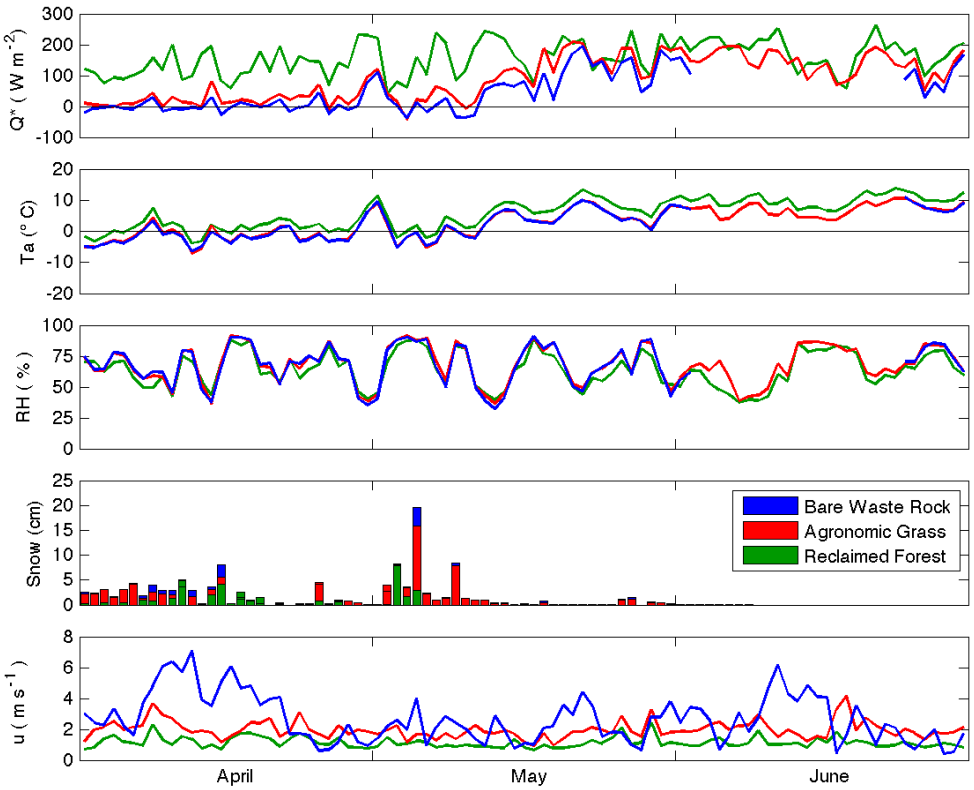

Figure 3.1: Ablation season (April 1 to June 30) daily average net radiation (Q*), air temperature (T_a), relative humidity (RH), daily cumulative snowfall (Snow) and wind speed (u) at each site.

	Recalimed Forest			Agronomic Grass			Bare Waste Rock		
	$\bar{x}$	SD	Range	$\bar{x}$	SD	Range	$\bar{x}$	SD	Range
Q* (W/m^2)	146.8	56.2	203.5	62.2	65.8	251.7	35.3	60.9	232.5
T_a (°C)	3.7	4.3	17.2	0.9	4.3	17.1	0.7	4.3	16.4
RH (%)	64.5	14	49.5	67.9	15.9	55.6	67.4	16.7	58.4
u (m/s)	1.2	0.4	1.8	1.9	0.5	2.7	2.7	1.6	6.5

Table 3.1: Average, standard deviation and range of climate variables; net radiation (Q*), air temperature (T_a), relative humidity (RH) and wind speed (*u*) for each research site. Values calculated for the period of April 1st to June 30th.

Q* was much greater at the reclaimed forest site compared to the agronomic grass and bare waste rock sites over the study period; and was 236% greater than the agronomic grass site and 415% greater than the bare waste rock site (Table 3.1; Figure 3.1). In mid May as snow melted and bare ground appeared, Q* values at the agronomic grass and bare waste rock sites increased to more closely match that of the reclaimed forest site (Figure 3.1). This pattern was due to the fact that the reclaimed forest site maintained a lower albedo due to the forest canopy resulting in less outgoing short-wave radiation (K↑). Q* inputs among sites became increasingly similar as snow surface cover decreased at the agronomic grass and bare waste-rock sites, resulting in increasingly similar albedo values among all sites.

3.2 Snow Surveys

Snow depth measurements as determined via the SR50A automated sonic sensor significantly underestimated the melt time at each site due to

rapid melting around the meteorological towers (Figure 3.2). To correct the continuous snow depth measurements to more accurately represent the observed snow depths during the ablation season, the SR50A snow depth for each site was corrected using the average snow depth from snow survey and snow pit data (Figure 3.3).

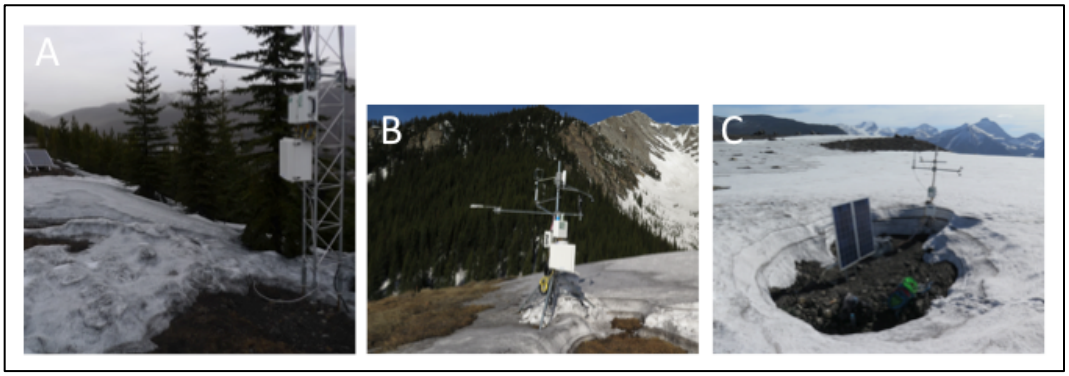

Figure 3.2: Early snowmelt at base of meteorological towers causing SR50A sensor error. Study sites; (a) Reclaimed Forest, (b) Agronomic Grass, (c) Bare Waste Rock. Photos taken in May 2014.

Study Site	Date of ablation start (obs)	Date of ablation start (model)	Date of snow removal (obs)	Date of snow removal (model)	Ablation duration (days; obs)	Ablation duration (days; model)	Calculated ablation rate (mm d^{-1}; obs)	Calculated ablation rate (mm d^{-1}; model)
Relaimed Forest	31-Mar	30-Mar	10-May	26-Apr	40	27	7.0	8.0
Agronomic Grass	06-May	19-Apr	04-Jun	04-Jun	29	46	22.4	11.3
Bare Waste Rock	11-May	19-Apr	09-Jun	05-Jun	29	47	24.1	12.5

Table 3.2: Observed and modelled ablation conditions at each site.

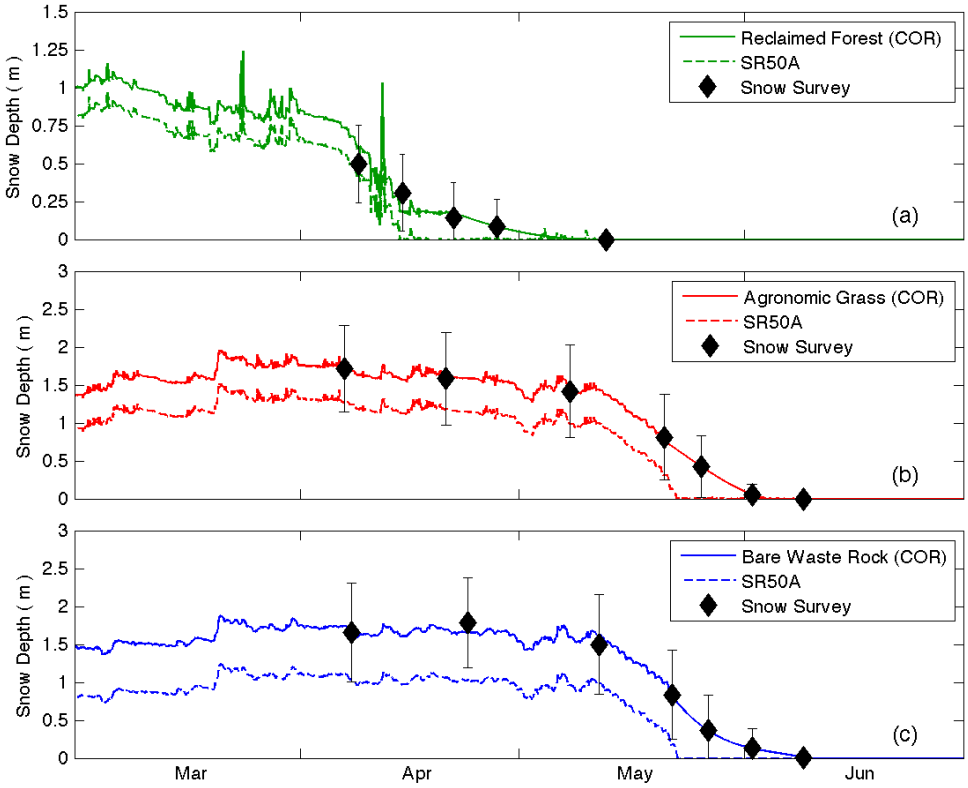

Figure 3.3: SR50A snow depth corrected for rapid melt at base of meteorological towers, using weekly snow surveys during 2014 ablation period. Error bars denote one standard deviation from the average.

The ablation season, defined as the date of measured peak SWE to the date the snowpack was completely removed (Dingman, 2002), varied at each of the three sites. The reclaimed forest ablation season was defined with a maximum SWE of 0.28 m on March 31, and was snow free on May 10, for a total ablation season of 40 days (Table 3.2). The agronomic grass site was defined with a maximum SWE of 0.65 m on May 6, and was snow free on June 4, for a total ablation season of 29 days. The bare waste rock site was defined with a maximum SWE of 0.70 m on May 11, and was snow free on June 9, for

a total ablation season of 29 days. Total snowfall for the reclaimed forest, agronomic grass and bare waste rock sites during their respective ablation seasons was 38.2, 94.1, and 107.9 cm. Other than a 0.04 m SWE increase on April 12 at the reclaimed forest site and a 0.03 m SWE increase on May 10 at the agronomic grass site, the ablation season was characterized by an extended period of positive daytime air temperatures during which ablation was continuous (Figure 3.4). Calculated ablation rates were lowest in the reclaimed forest site at 7 mm d^{-1} and greatest at the bare waste rock site at 24.1 mm d^{-1}, with the agronomic grass site 1.7 mm d^{-1} less than the bare waste rock site.

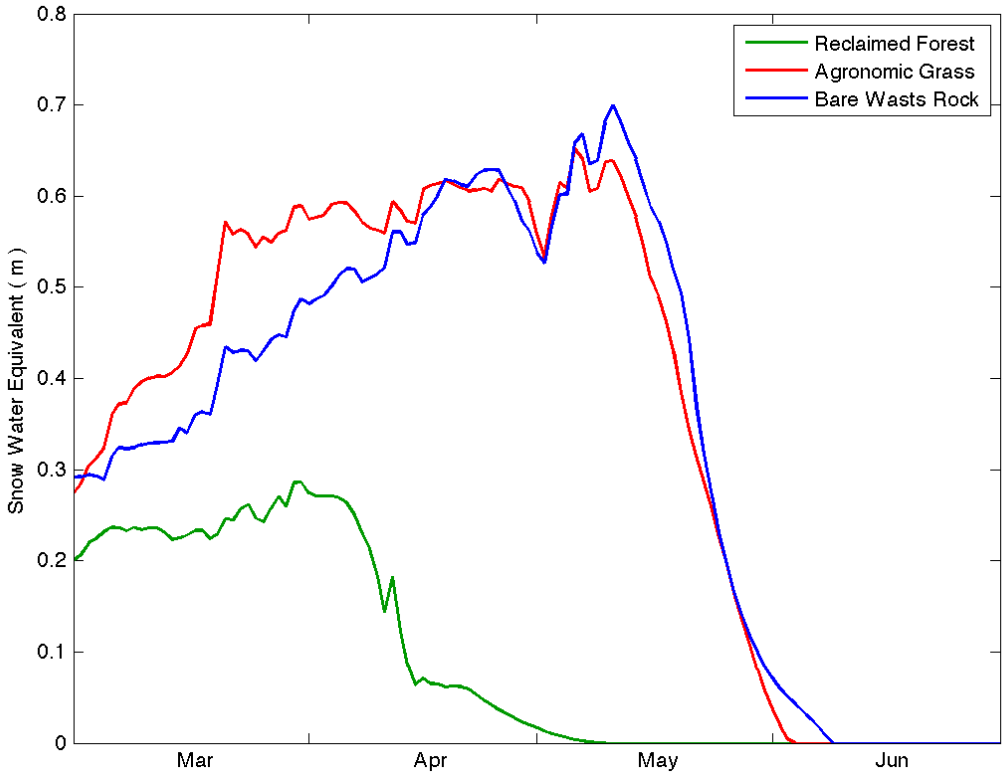

Figure 3.4: Measured snow water equivalent (SWE) during the 2014 ablation season.

3.3 Snow Energy Balance

Observed L* at the reclaimed forest and agronomic grass sites shows similar negative contributions of longwave energy (Figure 3.5). Values of K* at the reclaimed forest site are an order of magnitude greater than the agronomic grass site, but become more similar as albedo decreases at the agronomic grass site (Figure 3.5). K* is the most significant positive contributor to Q_m for the reclaimed forest, agronomic grass and presumably the bare waste rock site. Earlier positive contributions of *SHF* at the

reclaimed forest site are a result of above freezing temperatures occurring earlier than at the higher elevation sites (Figure 3.5). Beginning the week of May 19th, a reduction of subfreezing nighttime temperatures and an increase in daily sunlight hours resulted in an increase in the temperature gradient between the snow surface and the atmosphere, and a subsequent increase in the *SHF* contribution at the agronomic and bare waste rock sites. With increased temperatures and the subsequent increases in the vapour pressure gradients between the atmosphere and the snow surface the result is a minor increase of *LHF* (Figure 3.5). Due to site conditions resulting in an earlier ablation season, this increase in LHF occurs earlier at the reclaimed forest site.

Weekly average energy fluxes were calculated, with the week of April 9th representing a pre-ripened snowpack and the week of May 9th representing an isothermic snowpack (Figure 3.6). Q* is the dominant driver at the reclaimed forest site during both sample periods. Q* at the agronomic grass site is minimal during the April sampling period contributing only 16% to the Snow Energy Balance (SEB), however, during the May sampling period Q* is the dominant contributor to melt energy contributing 61% of the energy to the SEB (Table 3.3). This change in energy contribution at the agronomic grass site is the result of a continually decreasing albedo and a subsequent decrease in K↑, resulting in a greater positive contribution from K*. Negative values of Q* at the bare waste rock site for both sample periods are a result of

higher albedo values and solar shading due to the surrounding mountain peaks. The influence of turbulent fluxes remains similar at the reclaimed forest site, accounting for 34% of the SEB in April and 43% in May. At the agronomic grass site turbulent fluxes comprised 83% of the SEB in April, and only 1% in May. At the bare waste rock site, turbulent fluxes comprised 79% of the SEB in April and 61% in May. Decreases in turbulent flux contributions were attributed due to the reduction in wind velocity later in the ablation season and decreases in temperature and vapour pressure gradients. At all three sites GHF was a minor contributor to the SEB, contributing single digit negative values at the agronomic and bare waste rock sites for both sample periods, and 0% and 1% at the reclaimed forest site for the respective sample periods.

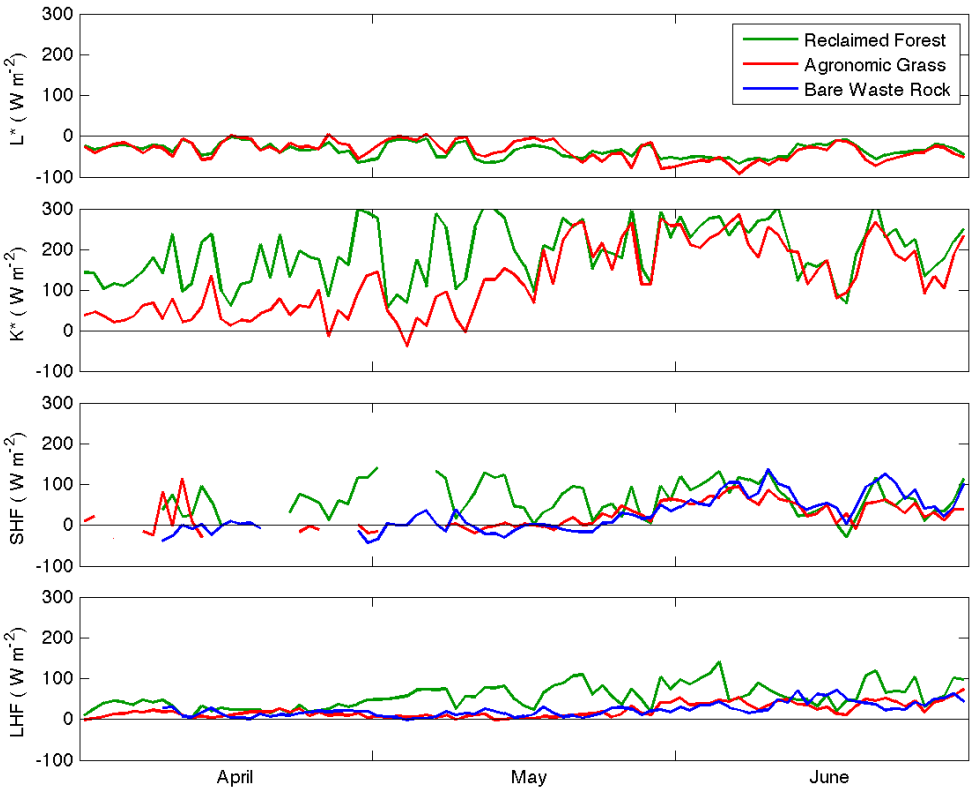

Figure 3.5: Daily average measured fluxes of, net long-wave radiation (L*), net short-wave radiation (K*), sensible heat (*SHF*) and latent heat (*LHF*) during the 2014 ablation period.

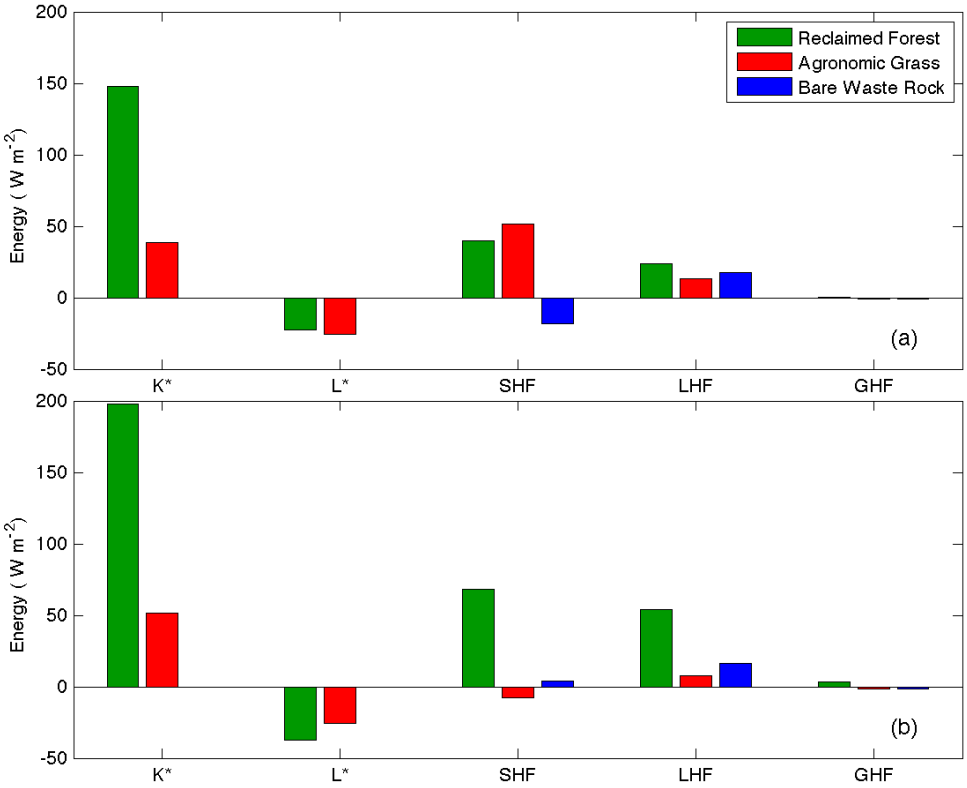

Figure 3.6: Weekly average energy fluxes; (a) week of April 9th representing a pre-ripened snowpack at the Agronomic and Waste Rock sites and an isothermic snowpack at the Reclaimed Forest Site, and (b) week of May 9th representing an isothermic snowpack at the Agronomic and Waste Rock sites and an output snowpack at the Reclaimed Forest site.

Study Site	*Q**	*SHF*	*LHF*	*GHF*
Reclaimed Forest	66%	21%	13%	0%
Agronomic Grass	16%	66%	17%	-1%
Bare Waste Rock	-20%	40%	39%	-1%

Week average energy fluxes, week of April 9 representing pre-ripened snowpack

Study Site	*Q**	*SHF*	*LHF*	*GHF*
Reclaimed Forest	56%	24%	19%	1%
Agronomic Grass	61%	-17%	18%	-4%
Bare Waste Rock	-34%	12%	49%	-5%

Week average energy fluxes, week of May 9 representing isothermic snowpack

Table 3.3: Weekly averages of energy flux contributions directed towards the snowpack, represented as percentages; net radiation (Q*), sensible heat (*SHF*) latent heat (*LHF*), ground heat (*GHF*).

3.4 Modelled vs. Measured Snow Cover and Snow Energy Balance

3.4.1 Snow Water Equivalent (SWE)

While it is difficult to compare absolute SWE values between records, the overall shape of the modelled SWE depletion curve corresponds well with corrected observed continuous SWE records (Table 3.4; Figure 3.7).

At the reclaimed forest site the model calculated a maximum SWE of 0.22 m, 78% of observed SWE and underestimated the date of snowpack removal by 14 days (Table 3.2). At the agronomic grass site the model calculated a maximum SWE of 0.52 m, 80% of observed SWE and model results and observed data gave the same date of snowpack removal. At the bare waste rock site the model calculated a maximum SWE of 0.59 m, 84% of observed SWE and underestimated the date of snowpack removal by 4 days. Underestimations of SWE by the SNOBALCRHM model at all three sites can be attributed to difficulties in modeling blowing snow and snow loading that was observed at each site during field visits and as observed in time-lapse imagery from each site.

Recalimed Forest	Agronomic Grass	Bare Waste Rock
0.91 (40)	0.94 (29)	0.94 (29)

Table 3.4: Observed versus modelled snow water equivalent (SWE). The r^2 value (n in days; $p < 0.001$) by research site.

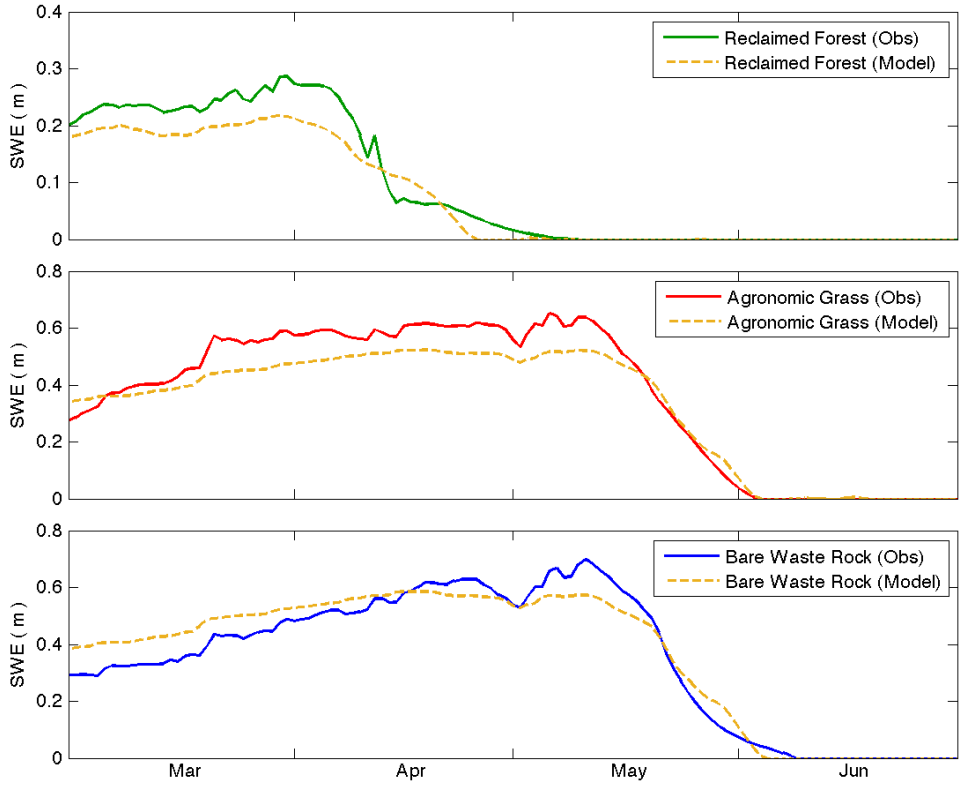

Figure 3.7: Observed and modelled snow water equivalent (SWE) during the 2014 ablation season.

3.4.2 Snow Energy Balance (SEB)

Measured and modelled Q* compared well at each of the three sites for the period from April 9th to April 16th for the reclaimed forest sites and May 9th to May 16th for the agronomic grass and bare waste rock sites (Table 3.5). The difference between modelled and measured Q* at the reclaimed forest and agronomic grass sites showed strong correspondence (Figure 3.8; Figure 3.9), with a coefficient of determination $r^2 = 0.98$ ($n = 337$, *P-value* <0.001) and $r^2 = 0.95$ ($n = 337$, *P-value* <0.001), respectively. The difference between

modelled and observed Q* at the bare waste rock site was greater than the other two sites, yet still statistically significant, with a coefficient of determination $r^2 = 0.77$ ($n = 337$, *P-value* <0.001). This lower coefficient of determination at the bare waste rock site can be attributed to an inverted representation of Q* between May 9th and May 12th (Figure 3.10). The model in all cases did a favourable job estimating nighttime Q* minimums, however, the model consistently underestimated the daily max Q* at all sites, resulting in MAE (W m^{-2}) for the reclaimed forest, agronomic grass and bare waste rock sites of 76 W m^{-2}, 26 W m^{-2} and 21 W m^{-2}, respectively.

	*Q**				*SHF*				*LHF*			
Study Site	**MAE** (W m^{-2})	**r^2**	***P-value***	**RMSE** (W m^{-2})	**MAE** (W m^{-2})	**r^2**	***P-value***	**RMSE** (W m^{-2})	**MAE** (W m^{-2})	**r^2**	***P-value***	**RMSE** (W m^{-2})
Relaimed Forest	110	0.98	< 0.001	179	76	0.05	0.3	121	28	0.01	0.9	47
Agronomic Grass	48	0.95	< 0.001	79	26	0.03	0.5	42	13	0.23	< 0.001	27
Bare Waste Rock	61	0.77	< 0.001	82	21	0.19	0.003	59	16	0.16	0.003	35

Table 3.5: Observed versus modelled net radiation (Q*), sensible heat (*SHF*) and latent heat (*LHF*).

Modelled *SHF* and *LHF* for a one week time period during each respected site's ablation period suggests that the physics of the energy exchange is not being adequately captured (Table 3.5). The coefficient of determination comparing the modelled and observed *SHF* for the reclaimed forest, agronomic grass and bare waste rock sites was $r^2 = 0.05$ ($n = 337$, *P-value* 0.3), $r^2 = 0.03$ ($n = 337$, *P-value* 0.5), $r^2 = 0.2$ ($n = 337$, *P-value* 0.003), respectively. The coefficient of determination values comparing LHF values

also demonstrate a low statistical relevance between the modelled and measured values, with $r^2 = 0.01$ (*n* = 337, *P-value* 0.9), $r^2 = 0.23$ (*n* = 337, *P-value* <0.001), $r^2 = 0.16$(*n* = 337, *P-value* 0.003) comparing the reclaimed forest, agronomic grass and bare waste rock sites, respectively. The model for the most part accurately represented nighttime fluxes of sensible and latent heat, however the model under-predicted the magnitude of daytime *SHF* and *LHF* (Table 3.6). Overall, there was a difference of 50, 0.9 and -3.6 W m^{-2} between measured and modelled *SHF* at the reclaimed forest, agronomic grass and bare waste rock sites, respectively (mean values (measured and modelled); 48.5 and -1.5 W m^{-2}, -4.4 and -5.3 W m^{-2}, -8.1 and -4.5 W m^{-2}, respectively). There was a difference of 20.4, -2.3 and 5.2 W m^{-2} between measured and modelled *LHF* at the reclaimed forest, agronomic grass and bare waste rock sites, respectively (mean values (measured and modelled); 25.3 and 4.9 W m^{-2}, 4.6 and 6.9 W m^{-2}, 14.6 and 9.4 W m^{-2}, respectively).

	SHF			***LHF***		
	obs	**model**		**obs**	**model**	
Study Site	**mean**	**mean**	**diff**	**mean**	**mean**	**diff**
Relaimed Forest	48.5	-1.50	50.00	25.3	4.9	20.4
Agronomic Grass	-4.4	-5.30	0.90	4.6	6.9	-2.3
Bare Waste Rock	-8.1	-4.50	-3.60	14.6	9.4	5.2

Table 3.6: Observed versus modelled sensible heat (*SHF*) latent heat (*LHF*), model performance of bulk transfer parameterization schemes.

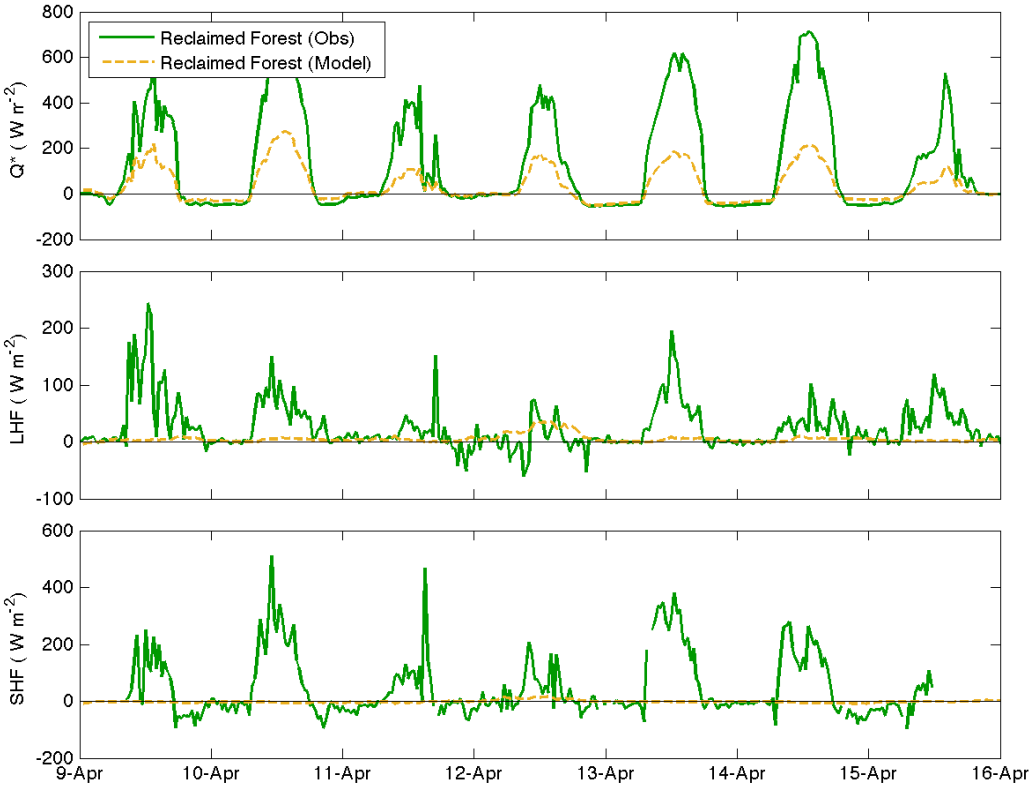

Figure 3.8: Reclaimed Forest observed and modelled daily average fluxes of, net radiation (Q*), sensible heat (*SHF*) and latent heat (*LHF*) for the week of April 9th to April 16th, representing an isothermic snowpack.

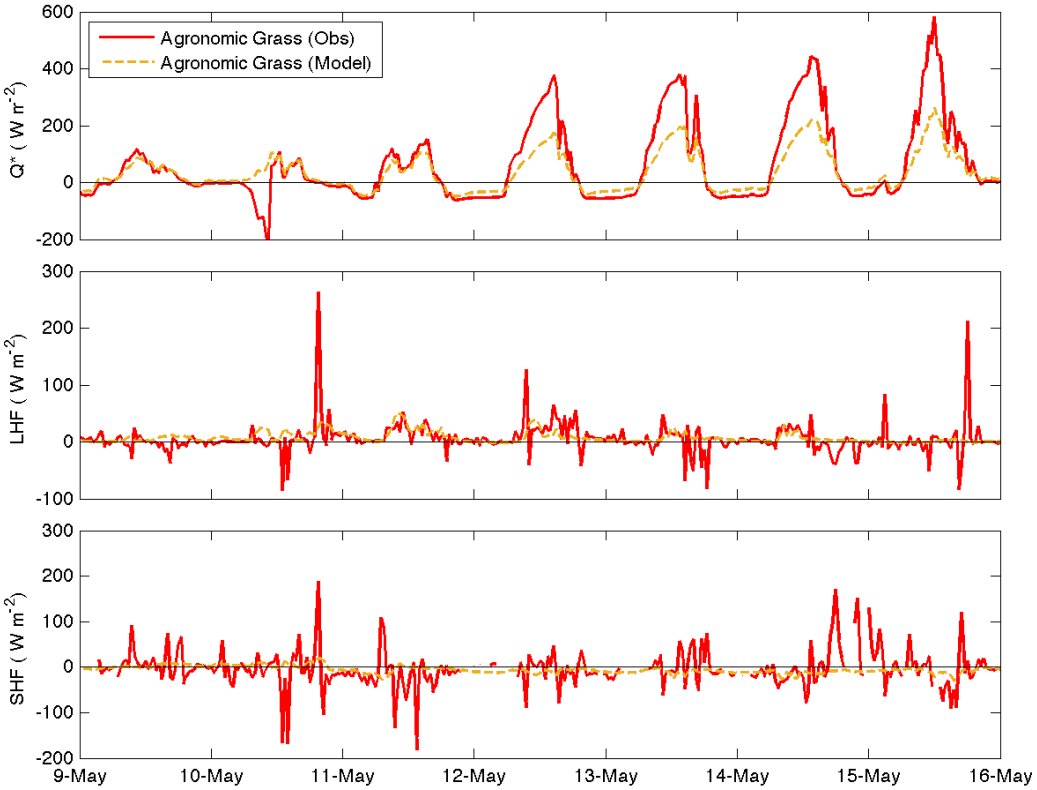

Figure 3.9: Agronomic Grass observed and modelled daily average fluxes of, net radiation (Q*), sensible heat (*SHF*) and latent heat (*LHF*) for the week of May 9th to May 16th, representing an isothermic snowpack.

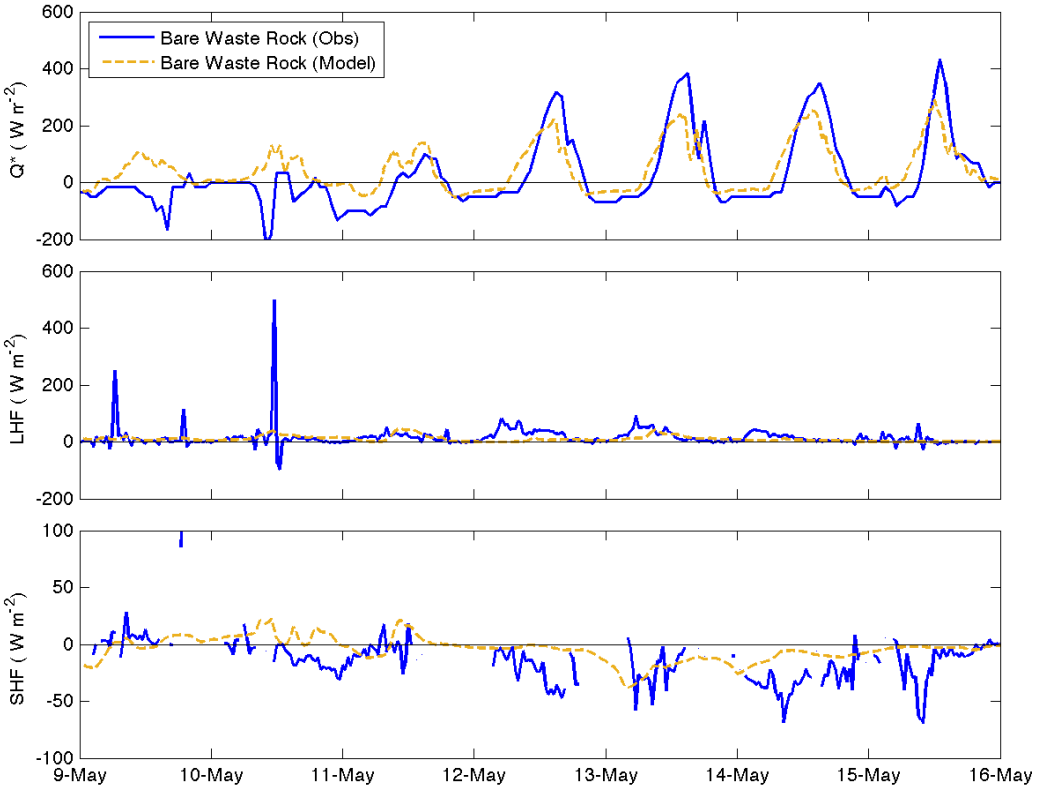

Figure 3.10: Bare Waste Rock observed and modelled daily average fluxes of, net radiation (Q*), sensible heat (*SHF*) and latent heat (*LHF*) for the week of May 9th to May 16th, representing an isothermic snowpack.

4.0 Discussion

Surface mining of coal in the Elk Valley, British Columbia utilizes a technique known as MTM/VF, a process by which surface vegetation is cleared and large volumes of waste rock are deposited in the valley bottoms in order to access the underlying coal formations, a process that forever alters the dynamics of the hydrological process within these watersheds. Minimal research has been conducted on how reclamation practices influence near surface water and energy partitioning atop waste rock in the Elk Valley (Nicholls et al., 2019), and there has been no direct evaluation of how reclamation practices affect snow accumulation and ablation on waste rock in this area. Considering levels of Se and other CI are directly correlated to the volume of water moving through coal spoils and the volume of waste rock in each spoil (Wellen et al., 2015, 2018), it is important to understand whether re-vegetation strategies can be used to minimize percolation into the coal spoils and subsequent chemical loading of streams and rivers from mined sites. Higher than background concentration of Se and other CI have already been reported downstream of mined catchments throughout the Elk Valley (Lussier et al., 2003). These elevated concentrations of Se and other CI create stressors to the aquatic biota living downstream and have the potential to negatively impact human health and recreation in the watershed (Chapman, P.M., Berdusco, R.J., Jones, 2007; Lussier et al., 2003; Wayland & Crosley, 2006).

The objectives of this study were threefold, 1) identify how site conditions and surface vegetation atop waste rock influence snow accumulation and ablation, 2) determine if processes of snow accumulation and ablation can be simulated using a physical based model and 3) determine if a physical based model can be used to model forest reclamation scenario testing. The following Discussion Chapter is divided into subsections addressing each of the three research objectives.

4.1 How site conditions and surface vegetation atop waste rock influence snow accumulation and ablation

2014 was an average year with regards to climate, receiving 98% of the annual snowpack compared to the 30-year normal and matching the average 30-year normal for temperature during the ablation season (Environment Canada, 2021). This climatically average year makes 2014 an ideal year to study how snow accumulation and ablation are influenced by site conditions and vegetation atop waste rock in the Elk Valley.

Elevation was the dominant control of snow accumulation among the three sites assessed during this study. The bare waste rock site located at an elevation of 2146 m a.s.l. accumulated the greatest maximum SWE of 0.70 m, followed by the agronomic grass site at an elevation of 2075 m a.s.l. with a maximum SWE of 0.65 m, and the reclaimed forest site at 1700 m a.s.l. accumulated the lowest maximum SWE of 0.28 m (Table 4.1). These results

correspond well with the literature (DeWalle & Rango, 2008; Dingman, 2002) and with previous studies of the region's annual temperature and precipitation lapse rates (Barbour et al., 2016; Shatilla, 2013).

Snow redistributed during the accumulation period accounted for approximately ± 10% of the maximum SWE for each site. At the agronomic grass and bare waste rock sites wind loading accounted for an additional 12% and 13% of the maximum SWE, respectively. At the reclaimed forest site, -9.3% of the maximum SWE was redistributed, presumably through canopy interception and redistribution, and sublimation from the canopy (Pomeroy et al., 2002; Schmidt et al., 1988). This indicates that a reclaimed forest atop waste rock reduces the SWE of that location. It can also be inferred that an agronomic grass surface has a negligible impact on snow accumulation.

Study Site	Max SWE (m)	Elevation (m a.sl.)	Precipitation Input (mm)	Precentage Input by Wind loading (%)
Relaimed Forest	0.28	1700	305.5	-9.3
Agronomic Grass	0.65	2075	570.5	12.3
Bare Waste Rock	0.70	2146	610.3	12.9

Table 4.1: Accumulation as a result of elevation and wind loading.

The date of total snowmelt varied by over a month among sites, with the reclaimed forest site becoming snow free on April 26 and the bare waste

rock site becoming snow free on June 9. Ablation rates were 69% and 71% lower at the reclaimed forest site than the agronomic grass and bare waste rock sites, respectively. These results correspond with studies that found ablation is 30-300% lower in live forest stands than in open areas (Boon, 2009; López-Moreno & Stähli, 2008; Murray & Buttle, 2003; Pomeroy & Granger, 1997; Spittlehouse & Winkler, 2005). The agronomic grass site, however, shows minimal difference in snow ablation relative to the bare waste rock site; thus, it can be assumed that a waste rock surface reclaimed with agronomic grass species has little influence on snow ablation rates compared to an unreclaimed bare waste rock surface. Without a lysimeter at each site to compare differences in snowmelt percolation, this study is unable to comment on the impact vegetation could have on net percolation into the coal spoil. For future research, the addition of lysimeters at each site would help to address the influence of vegetation on net percolation.

Ablation at the reclaimed forest and agronomic grass sites was driven largely by K↓, although turbulent flux contributions at the reclaimed forest site were substantial. K↓ as the dominant driver of ablation in mountain environments and its subsequent contribution to Q* is well documented in the literature (Koivusalo & Kokkonen, 2002; Spittlehouse & Winkler, 2005; Winkler & Boon, 2014), and is further supported by results from this study. The 43% contribution of turbulence fluxes to ablation at the reclaimed forest site (Table 3.3) is somewhat counter to the literature that found turbulent

fluxes play a minor role in ablation in a forest plot (Boon, 2009). Results of larger than expected contributions from turbulent fluxes at the reclaimed forest site were attributed to unvegetated waste rock upwind of the treed site and significant spacing between trees, increasing the surface roughness thus generating more turbulence compared to that of a natural forest. At the bare waste rock site, ablation was driven largely by turbulent fluxes, with LHF contributing almost half of the total melt energy. Large contributions to melt energy from turbulent fluxes at the bare waste rock site compares well to studies comparing ablation rates of clear cut and forested plots (Boon, 2007; Burles & Boon, 2011; Winkler & Boon, 2014). Negative values of Q* at the bare waste rock site are attributed to higher albedo values and solar shading due to the surrounding mountain peaks.

A number of studies have assessed how natural and anthropogenic changes to vegetation in mountain environments impact snow accumulation and ablation (Boon, 2009, 2012; Dixon, Boon, & Silins, 2014; John Pomeroy et al., 2012; Winkler & Boon, 2014), however, no study to this author's knowledge has specifically studied how site conditions and surface vegetation atop waste rock influence snow accumulation and ablation. The practical application of these results suggest reclaiming a bare waste rock surface with trees will reduce the total SWE of that area, therefore, reducing the amount of water percolating through the coal spoil and subsequent rock-water interactions. The ability of the reclaimed forest to reduce daily ablation

rates and prolong the ablation period could reduce the flashiness of the watershed and reduce Se loading by staggering water vertically percolating through preferential flow paths with low water-rock interaction, however, this topic of study would require further research. The application of a reclaimed forest to potentially reduce Se is further supported by Wellen et al. (2015), who suggested, "reclamation as represented by surface re-vegetation has some potential to become a Se management tool". Results from this study also suggest a strategic focus to reclamation could be applied to areas with a higher SWE potential. Under these parameters reclamation should prioritize upper elevations and areas prone to snow loading.

4.2 Processes of snow accumulation and ablation can be simulated using a physical based model

Overall, results show that SNOBALCRHM was able to represent the quantity and timing of snow accumulation and ablation at a reclaimed forest, agronomic grass and bare waste rock sites. Acceptable results were achieved in terms of characterizing the differences in snow accumulation and ablation observed between the three sites. Despite the poor representation of turbulent fluxes (Table 3.6) the physical basis of SNOBALCRHM is sufficient to represent snow processes of a reclaimed forest, agronomic grass and bare waste rock sites. Model results were sensitive to parameters of quantifying vegetation cover and blowing snow.

Modelled mean and maximum SWE exhibited low systematic bias at the reclaimed forest, agronomic grass and bare waste rock sites. This suggests that much of the errors incurred were random in nature, resulting from either model parameterization or observations (Ellis et al., 2010). The poorest model results of SWE occurred at the reclaimed forest site, which underestimated the maximum SWE by 22% and underestimated the date of snowpack removal by 14 days. Such results may not be unexpected, as the reclaimed forest site had significantly lower accumulations relative to the agronomic and bare waste rocks sites, plus, the added complexity and potential for error that vegetation adds to the model parameters. Previous applications of SNOBALCRHM have shown that shallower snowpacks are more sensitive to simulation errors of mass and energy, therefore, a potential source of larger relative errors, and that forest vegetation dramatically decreases the model's predictive capability (Ellis et al., 2010; Pomeroy et al., 2012).

The model consistently underestimated SWE values at all three sites, with poorer predictions occurring during the accumulation periods (Figure 3.7). These discrepancies in SWE values between the modelled and observed values were attributed to the models inefficiency at simulating blowing snow and snow loading in a complex post mined mountain landscape. During the ablation season, reduced wind speeds and heavier, more consolidated snow attributed to a reduction in wind redistribution of snow and a reduction in

the resulting model error. As such, improvement in SNOBALCRHM's representation of blowing snow or better model calibration may be required to more closely represent parameters of blowing snow.

Results show the model represented the total energy to the snowpack and the relative contributions of most individual energy terms. SNOBALCRHM was able to represent net radiation at all three sites; however, the model's predictive ability regarding turbulent fluxes requires improvement. Errors in estimating longwave and shortwave radiation were small and resulted in accurate estimations of Q* at each site. Despite modelled and observed mean values of *LHF* and *SHF* being within a tolerable range for the agronomic grass and bare waste rock sites (Table 3.4), the model output for turbulent fluxes was often an inverted value to the observed and underrepresented the degree of magnitude of diurnal flux patterns. At the reclaimed forest site, modelled results of turbulent fluxes are even less correlated. This decrease in the model's predictive capability of net radiation and total energy to the snowpack is associated with tree cover, as seen in the decreasing model efficiency with the increasing number of combined energy terms (Ellis et al., 2010).

Despite some uncertainty in model performance, results show SNOBALCRHM is capable of providing a good characterization of critical snow processes at a reclaimed forest, agronomic grass and bare waste rock sites, with only modest requirements for meteorological forcing data and site

information. Results from this study encourage the use of SNOBALCRHM as a diagnostic tool in a post mined environment, which is exemplified by the representation of the dramatic differences in the snow accumulation and ablation observed between the reclaimed forest and the other two research sites. There is additional confidence in SNOBALCRHM's potential to represent snow accumulation and ablation by site conditions and vegetation atop waste rock, as simulations weren't calibrated to any objective function. Therefore, modelled results could be improved with greater calibration of meteorological data and model parameterization.

The practical application of these results shows SNOBALCRHM is capable of representing the effects on snow accumulation and ablation brought about by changes in vegetation cover, topography and substrate as a result of MTM/VF activities. And that SNOBALCRHM shows promise as a diagnostic tool that could be incorporated into larger, more long-term studies of mine operations and their impacts on Se loading, as snow would be an important factor to account for in long-term mine operation plans.

4.3 A physical based model can be used to model forest reclamation scenario testing

Results from this and previous work (Ellis et al., 2010; Pomeroy et al., 2007; Pomeroy et al., 2012) are encouraging for the use of SNOBALCRHM as not only a diagnostic tool, but a predictive tool in investigating reclamation

effects on snow processes in a post MTM/VF landscape. Based on the statistical relevance of the model's predictive SWE values compared to the observed values ($r^2 > 0.9$; $p < 0.001$), SNOBALCRHM shows its effectiveness at estimating SWE during the accumulation and ablation periods. It can therefore be assumed that if SNOBALCRHM can accurately model observed snow processes and SWE values, it can be used to make reasonable SWE predictions of reclamation scenarios.

To emphasize the potential of SNOBALCRHM as a scenario-testing tool, a simulated forest was added to the agronomic grass site. The simulated forest mimicked the needleaf vegetation parameters at the reclaimed forest site, with a LAI of 2.79 m^2 m^{-2} and a tree height of 6 m. The remaining site information and meteorological forcing data remained the same as that observed at the agronomic grass site in 2014.

With the addition of the simulated forest at the agronomic grass site SNOBALCRHM calculated a maximum SWE of 0.20 m, 31% of the observed 0.65 m SWE and 39% of the modelled 0.52 m SWE (Figure 4.1). The modelled result of a simulated forest at the agronomic grass site had an ablation start date of April 17 and was calculated to be snow free on May 25, for a total ablation duration of 39 days. These results are closely aligned with observed results from the reclaimed forest site, which had a maximum SWE of 0.28 m and an ablation period of 40 days. The 18 day difference between the reclaimed forest's ablation start date of March 31 and the ablation start date

of the simulated forest at the agronomic grass site can be explained by the regional adiabatic lapse rate and the resulting prolonged colder temperatures at the higher elevation site. Results are further supported by the calculated ablation rates, with the simulated forest at the agronomic grass site again showing a similar ablation rate of 5 mm d^{-1} compared to the observed ablation rate at the reclaimed forest of 7 mm d^{-1}.

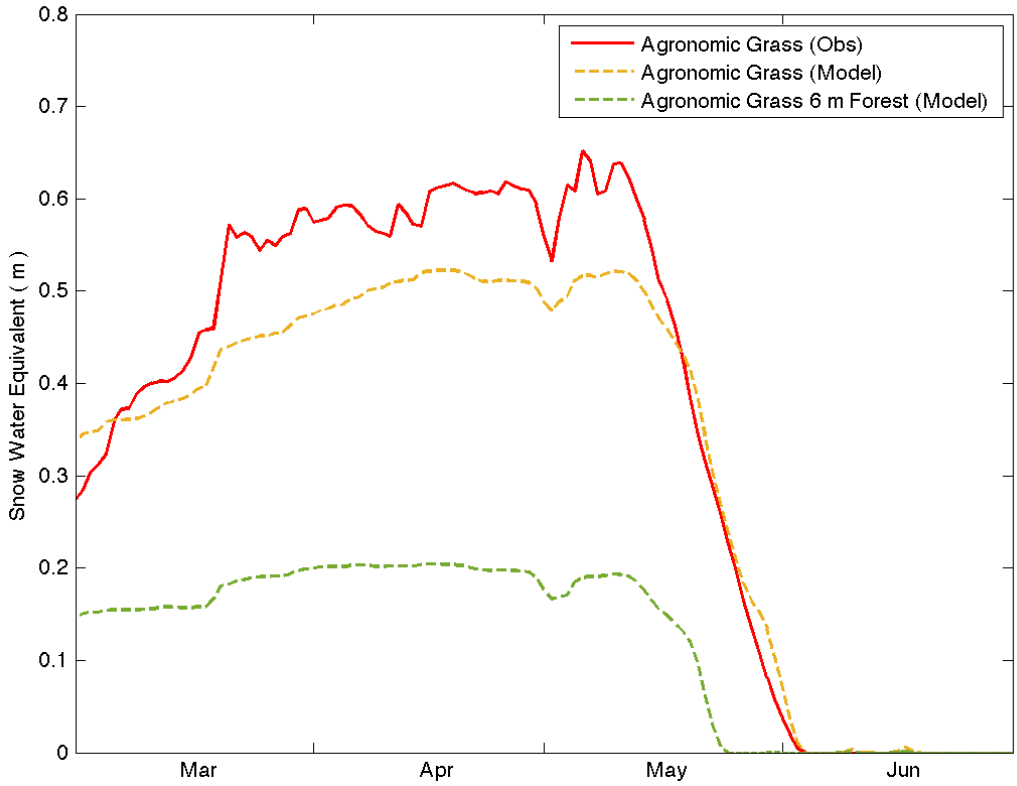

Figure 4.1: Snow water equivalent (SWE) model scenario test at the Agronomic Grass site with the addition of a simulated needleleaf forest, with a leaf area index (LAI) of 2.79 m^2 m^{-2} and a mean tree height of 6 m, compared to observed and modelled SWE values during the 2014 ablation season.

Contributions of Q* to the total melt energy of the simulated forest at the agronomic grass site shows reasonable predictions, with Q* representing 51% of the April pre-ripened snowpack SEB and 49% of the May isothermic snowpack SEB. These predictions of Q* compare well with observed contributions of Q* at the reclaimed forest site for the same dates (Table 3.3), and are a good match to Q* contributions to the SEB in needleleaf forests from other research (Boon, 2009; Burles & Boon, 2011). Similar to results in this study comparing observed and modelled values of turbulent fluxes, SNOBALCRHM's predictions of turbulent fluxes in a simulated forest are the inverse of what was observed in this study and what was previously reported in the literature (Boon, 2009; DeWalle & Rango, 2008; Dingman, 2002). With the addition of the simulated forest, turbulent fluxes contributed -31% to the SEB in the April pre-ripened snowpack and -1% of the SEB in the May isothermic snowpack, compared to 34% and 43% contributions observed at the reclaimed forest site and 83% and 1% observed a the agronomic grass site, for the same respective dates. Modelled turbulent flux predictions in a simulated forest at the agronomic grass site require further analysis and calibration to create a more representative prediction of the physical processes. SNOBALCRHM's prediction of Q*m* at a simulated forest provides insight into the significant potential impacts a mature needleleaf forest could have, with the model predicting a 65% decrease in melt energy with the addition of a simulated 6 m forest. This predicted discrepancy in Q*m* due to

the addition of a simulated forest is comparable to changes in Q*m* that have been documented in previous research comparing mature forests to clearcut sites (Boon, 2007; Dixon et al., 2014; Winkler & Boon, 2014).

This study assessed the ability of SNOBALCRHM, a physical based model, to simulate processes of snow accumulation and ablation, and the models potential for forest reclamation scenario testing. Good results in the models predictive SWE values for the reclaimed forest, agronomic grass and bare waste rock sites, as well as, the reasonable prediction of SWE in a simulated forest scenario shows SNOBALCRHM has promise as a scenario testing tool in a post MTM/VF landscape and further research and calibration would result in more accurate predictive outcomes.

The practical application of SNOBALCRHM as a reclamation scenario testing tool and as a forest disturbance scenario testing tool for MTM/VF practices in the Elk Valley, would help to better understand the influence of vegetation on snow accumulation and ablation, and the subsequent infiltration of snowmelt into the coal spoil. Based on the preliminary scenario of adding a 6 m forest to the agronomic grass site we see a reduction of 0.45 m SWE, perceivably due to precipitation interception from the canopy resulting in increased loses of snow due to sublimation and re-suspension (Harding & Pomeroy, 1996; Pomeroy & Gray, 1995; Pomeroy & Parviainen, 1998). With only 31% of the snow accumulating at the agronomic grass site under this reclamation scenario, it can be assumed that the amount of water

leaving this site through infiltration and surface runoff would decrease by a similar ratio. These results demonstrate the substantial influence reclamation practices could have on the catchment hydrology, influencing snow accumulation and melt, as well as the reduction in hydrological and geochemical influences from MTM/VF coal mining practices. More work is needed to understand how snowmelt infiltration impacts the CI issue downstream of the coal spoil and how reclamation practices could help mitigate this problem. However, SNOBALCRHM as a scenario-testing tool shows promise in helping to further answer these complex questions.

5.0 Conclusion

In this study, snow accumulation and ablation, meteorological data and site conditions were measured, modelled and compared at three sites in 2014; a reclaimed forest site with ~35 year-old mixed conifer trees, a reclaimed site planted with agronomic grass species and a bare waste rock site. The specific objectives of this study were to 1) identify how site conditions and surface vegetation atop waste rock influence snow accumulation and ablation, 2) determine if processes of snow accumulation and ablation can be simulated using a physical based model and 3) determine if a physical based model can be used to model forest reclamation scenario testing.

Results show that elevation was the dominant factor for snow accumulation among sites, with the bare waste rock receiving the greatest SWE, followed by the agronomic grass and reclaimed forest sites, respectively. The date of snowmelt varied by over a month among sites, with the reclaimed forest site becoming snow free on April 26 and the bare waste rock site becoming snow free on June 9. Ablation was driven largely by incoming shortwave radiation although turbulent fluxes were substantial. Ablation rates were 69% and 71% lower at the reclaimed forest site than the agronomic grass and bare waste rock sites, respectively. Overall, results show that SNOBALCRHM was able to accurately represent the quantity and timing of snow accumulation and ablation at a reclaimed forest, agronomic

grass and bare waste rock sites. Model results were sensitive to parameters of quantifying vegetation cover and blowing snow. Despite some uncertainty in SNOBALCRHM's performance, results from this study encourage the use of SNOBALCRHM as a forest reclamation scenario-testing tool. Although these results suggest planting trees atop waste rock will reduce net percolation through coal spoil and the subsequent chemical loading, results are confined to the winter season, and a more comprehensive study of the water balance is required in this hydrologically complex mountain environment.

References

Bailey, R. T., Gates, T. K., & Halvorson, A. D. (2013). Simulating variably-saturated reactive transport of selenium and nitrogen in agricultural groundwater systems. *Journal of Contaminant Hydrology*, *149*. https://doi.org/10.1016/j.jconhyd.2013.03.001

Barbour, S. L., Hendry, M. J., & Carey, S. K. (2016). High-resolution profiling of the stable isotopes of water in unsaturated coal waste rock. *Journal of Hydrology*, *534*, 616–629. https://doi.org/10.1016/j.jhydrol.2016.01.053

Barnett, T. P., Adam, J. C., & Lettenmaier, D. P. (2005). Potential impacts of a warming climate on water availability in snow-dominated regions. *Nature*. https://doi.org/10.1038/nature04141

Becker, A. (2005). Runoff Processes in Mountain Headwater Catchments: Recent Understanding and Research Challenges. https://doi.org/10.1007/1-4020-3508-x_29

Bernhardt, E. S., Lutz, B. D., King, R. S., Fay, J. P., Carter, C. E., Helton, A. M., … Amos, J. (2012). How many mountains can we mine? Assessing the regional degradation of central appalachian rivers by surface coal mining. *Environmental Science and Technology*, *46*(15). https://doi.org/10.1021/es301144q

Boon, S. (2007). Northern Interior British Columbia. *BC Journal of Ecosystem and Management*, *8*(3), 1–13.

Boon, S. (2009). Snow ablation energy balance in a dead forest stand. *Hydrological Processes*, *2610*(January), 2600–2610. https://doi.org/10.1002/hyp

Boon, S. (2012). Snow accumulation following forest disturbance. *Ecohydrology*, *5*(3). https://doi.org/10.1002/eco.212

Bray, D. I. (1973). REPORT ON THE VARIABILITY OF SNOW WATER EQUIVALENT MEASUREMENTS AT A SITE.

Burles, K., & Boon, S. (2011). Snowmelt energy balance in a burned forest plot, Crowsnest Pass, Alberta, Canada. *Hydrological Processes*, *25*(19). https://doi.org/10.1002/hyp.8067

Chang, M. (2013). *Forest hydrology. An introduction to water and forest, Third Edition*. *Floods in a Changing Climate: Extreme Precipitation*.

Chapman, P.M., Berdusco, R.J., Jones, R. (2007). *Update on the status of selenium investigations in the Elk River Valley, B.C.*

Colbeck, S. C. (1982). An overview of seasonal snow metamorphism. *Reviews of Geophysics*. https://doi.org/10.1029/RG020i001p00045

DeBeer, C. M., & Pomeroy, J. W. (2010). Simulation of the snowmelt runoff contributing area in a small alpine basin. *Hydrology and Earth System Sciences*, *14*(7), 1205–1219. https://doi.org/10.5194/hess-14-1205-

2010
Dessouki, T., & Ryan, A. (2010). *Canada–British Columbia water quality monitoring agreement: Water quality assessment of the Kootenay, Elk, and Mary Rivers*. Victoria, British Columbia.
DeWalle, D. R., & Rango, A. (2008). *Principles of snow hydrology*. *Principles of Snow Hydrology* (Vol. 9780521823623). https://doi.org/10.1017/CBO9780511535673
Dickens, P. S., Minear, R. A., & Tschantz, B. A. (2012). Hydrologic alteration of mountain watersheds from surface mining. *Journal - Water Pollution Control Federation*, *61*(7), 1249–1260. Retrieved from http://cat.inist.fr/?aModele=afficheN&cpsidt=7342431
Diehl, S. F., Goldhaber, M. B., Koenig, A. E., Lowers, H. A., & Ruppert, L. F. (2012). Distribution of arsenic, selenium, and other trace elements in high pyrite Appalachian coals: Evidence for multiple episodes of pyrite formation. *International Journal of Coal Geology*, *94*. https://doi.org/10.1016/j.coal.2012.01.015
Dingman, S. L. (2002). *Physical Hydrology* (2nd ed.). Upper saddle River, New Jersey: Prentice Hall.
Dixon, D., & Boon, S. (2012). Comparison of the SnowHydro snow sampler with existing snow tube designs. *Hydrological Processes*, *26*(17), 2555–2562. https://doi.org/10.1002/hyp.9317
Dixon, D., Boon, S., & Silins, U. (2014). Watershed-scale controls on snow accumulation in a small montane watershed, southwestern Alberta, Canada. *Hydrological Processes*, *28*(3), 1294–1306. https://doi.org/10.1002/hyp.9667
Ellis, C. R., Pomeroy, J. W., Brown, T., & MacDonald, J. (2010). Simulation of snow accumulation and melt in needleleaf forest environments. *Hydrology and Earth System Sciences*, *14*, 925–940. https://doi.org/10.5194/hess-14-925-2010
Ellis, C. R., Pomeroy, J. W., & Link, T. E. (2013). Modeling increases in snowmelt yield and desynchronization resulting from forest gap-thinning treatments in a northern mountain headwater basin. *Water Resources Research*, *49*(2), 936–949. https://doi.org/10.1002/wrcr.20089
Environment Canada. (2021). Canadian Climate Normals, 1981-2010 station data Sparwood. Retrieved November 16, 2021, from https://climate.weather.gc.ca/climate_normals/results_1981_2010_e.html?stnID=1207&autofwd=1
Falge, E., Baldocchi, D., & Olson, R. (2001). Gap filling strategies for defensible annual sums of net ecosystem exchange. *Agricultural and Forest …*, *107*, 43–69. Retrieved from http://www.sciencedirect.com/science/article/pii/S0168192300002252

Flerchinger, G. (2000). *The simultaneous heat and water (SHAW) Model: Technical Documentation*. USDA Agricultural Research Service, Boise, Idaho.

Gelfan, A., Pomeroy, J. W., & Kuchment, L. S. (2004). Modeling forest cover influences on snow accumulation, sublimation, and melt. *Journal of …*, (1997), 785–803. Retrieved from http://search.ebscohost.com/login.aspx?direct=true&profile=ehost&scope=site&authtype=crawler&jrnl=1525755X&AN=14910357&h=AJUupZEBwKMJbz3DPsEf5LKzmJPZYab2xgVC02iTpPJQBcHLG0Y8sOxtR1D9njuGYN9rCpiK2t0PDtyod9TFYQ%253D%253D&crl=c

Golding, D. L., & Swanson, R. H. (1986). Snow distribution patterns in clearings and adjacent forest. *Water Resources Research*, *22*(13). https://doi.org/10.1029/WR022i013p01931

Gray, D., & Landine, P. (1987). Albedo model for shallow prairie snow covers. *Canadian Journal of Earth Sciences*, (1973). Retrieved from http://www.nrcresearchpress.com/doi/abs/10.1139/e87-168

Gray, D., & Landine, P. (1988). An energy-budget snowmelt model for the Canadian Prairies. *Canadian Journal of Earth Sciences*, (1978). Retrieved from http://www.nrcresearchpress.com/doi/abs/10.1139/e88-124

Griffith, M. B., Norton, S. B., Alexander, L. C., Pollard, A. I., & LeDuc, S. D. (2012). The effects of mountaintop mines and valley fills on the physicochemical quality of stream ecosystems in the central Appalachians: A review. *Science of the Total Environment*. https://doi.org/10.1016/j.scitotenv.2011.12.042

Hanna, R. B., & Loftis, J. C. (2007). Load Modeling Approach for Evaluating Selenium Stream Standards Compliance. *Journal of Irrigation and Drainage Engineering*, *133*(3). https://doi.org/10.1061/(asce)0733-9437(2007)133:3(232)

Harding, R., & Pomeroy, J. (1996). Energy Balance of the Winter Boreal Landscape. *Journal of Climate*. Retrieved from http://journals.ametsoc.org/doi/abs/10.1175/1520-0442(1996)009%253C2778:TEBOTW%253E2.0.CO;2

Hardy, J. P., Groffman, P. M., Fitzhugh, R. D., Henry, K. S., Welman, A. T., Demers, J. D., … Nolan, S. (2001). Snow depth manipulation and its influence on soil frost and water dynamics in a northern hardwood forest. *Biogeochemistry*, *56*(2). https://doi.org/10.1023/A:1013036803050

Hedstrom, N., & Pomeroy, J. (1998). Measurements and modelling of snow interception in the boreal forest. *Hydrological Processes*, *1625*(March), 1611–1625. Retrieved from http://www.usask.ca/hydrology/papers/Hedstrom_Pomeroy_1998.pdf

Helie, J. F., Peters, D. L., Tattrie, K. R., & Gibson, J. J. (2005). Review and Synthesis of Potential Hydrologic Impacts of Mountain Pine Beetle and

Related Harvesting Activities in British Columbia. *Mountain Pine Beetle Initiative Working Paper*.

Hendryx, M. S., Lemly, A. D., Likens, G. E., Loucks, O. L., Power, M. E., White, P. S., & Wilcock, P. R. (2010). Mountaintop Mining Consequences. *Science*, *327*, 148–149. https://doi.org/10.1126/science.1180543

Herrmann, H., & Bucksch, H. (2014). Handbook of Hydrology. In *Dictionary Geotechnical Engineering/Wörterbuch GeoTechnik*. https://doi.org/10.1007/978-3-642-41714-6_80111

Hock, R., Rees, G., Williams, M. W., & Ramirez, E. (2006). Contribution from glaciers and snow cover to runoff from mountains in different climates. *Hydrological Processes*. https://doi.org/10.1002/hyp.6206

Hoeg, S., Uhlenbrook, S., & Leibundgut, C. (2000). Hydrograph separation in a mountainous catchment - combining hydrochemical and isotopic tracers. *Hydrological Processes*, *14*(7). https://doi.org/10.1002/(SICI)1099-1085(200005)14:7<1199::AID-HYP35>3.0.CO;2-K

Horst, T. W. (1997). A simple formula for attenuation of eddy fluxes measured with first-order-response scalar sensors. *Boundary-Layer Meteorology*, *82*(2). https://doi.org/10.1023/A:1000229130034

Huang, S. S. Y., Strathe, A. B., Hung, S. S. O., Boston, R. C., & Fadel, J. G. (2012). Selenocompounds in juvenile white sturgeon: Estimating absorption, disposition, and elimination of selenium using Bayesian hierarchical modeling. *Aquatic Toxicology*, *109*, 150–157. https://doi.org/10.1016/j.aquatox.2011.11.005

IEG Consultants Ltd. (2013). *IEG TRCWRA-13_CSP_Forest Data V3*. Calgary.

Jayaweera, G. R., & Biggar, J. W. (1996). Role of Redox Potential in Chemical Transformations of Selenium in Soils. *Soil Science Society of America Journal*, *60*(4). https://doi.org/10.2136/sssaj1996.03615995006000040014x

Jonas, T., Marty, C., & Magnusson, J. (2009). Estimating the snow water equivalent from snow depth measurements in the Swiss Alps. *Journal of Hydrology*, *378*(1–2), 161–167. https://doi.org/10.1016/j.jhydrol.2009.09.021

Kennedy, C., Day, S., Macgregor, D., & Pumphrey, J. (2012). Selenium Leaching from Coal Waste Rock in the Elk Valley , B . C . *9th International Conference on Acid Rock Drainage*, (January 2012), 1690–1702.

Koivusalo, H., & Kokkonen, T. (2002). Snow processes in a forest clearing and in a coniferous forest. *Journal of Hydrology*, *262*(1–4). https://doi.org/10.1016/S0022-1694(02)00031-8

Lillquist, Karl; Walker, K. (2006). Historical Glacier and Climate Fluctuations at Mount Hood, Oregon. Arctic Antarctic and Alpine Research. In *ARCT ANTARCT ALP RES* (pp. 399–412).

Lindberg, T. T., Bernhardt, E. S., Bier, R., Helton, A. M., Brittany Merola, R.,

Vengosh, A., & Di Giulio, R. T. (2011). Cumulative impacts of mountaintop mining on an Appalachian watershed. *Proceedings of the National Academy of Sciences of the United States of America*, *108*(52). https://doi.org/10.1073/pnas.1112381108

Link, T. E., & Marks, D. (1999). Point simulation of seasonal snow cover dynamics beneath boreal forest canopies. *Journal of Geophysical Research Atmospheres*, *104*(D22), 27841–27857. https://doi.org/10.1029/1998JD200121

Liston, G. E., & Sturm, M. (2002). Winter precipitation patterns in arctic Alaska determined from a blowing-snow model and snow-depth observations. *Journal of Hydrometeorology*, *3*(6). https://doi.org/10.1175/1525-7541(2002)003<0646:WPPIAA>2.0.CO;2

López-Moreno, J. I., & Stähli, M. (2008). Statistical analysis of the snow cover variability in a subalpine watershed: Assessing the role of topography and forest interactions. *Journal of Hydrology*, *348*(3–4). https://doi.org/10.1016/j.jhydrol.2007.10.018

Lussier, C., Veiga, V., & Baldwin, S. (2003). The Geochemistry of Selenium Associated with Coal Waste in the Elk River Valley, Canada. *Environmental Geology*, *44*(8), 905–913. https://doi.org/10.1007/s00254-003-0833-y

Male, D. H., & Gray, D. M. (1981). Handbook of Snow. *Handbook of Snow*, 338–358.

Marks, D., & Dozier, J. (1992). Climate and energy exchange at the snow surface in the Alpine Region of the Sierra Nevada: 2. Snow cover energy balance. *Water Resources Research*, *28*(11), 3043–3054. https://doi.org/10.1029/92WR01483

Marks, D., Dozier, J., & Davis, R. (1992). Climate and energy exchange at the snow surface in the alpine region of the Sierra Nevada: 1. Meteorological measurements and monitoring. *Water Resources Research*, *28*(92), 3029–3042. Retrieved from http://onlinelibrary.wiley.com/doi/10.1029/92WR01482/full

Marks, D., Kimball, J., Tingey, D., & Link, T. (1998). The sensitivity of snowmelt processes to climate conditions and forest cover during rain-on-snow: a case study of the 1996 Pacific Northwest flood. *Hydrol. Process*, *1587*(March), 1569–1587.

Martinec, J., Rango, A., & Major, E. (1983). The snowmelt- runoff model (SRM) user's manual.

Miller, A., & Zégre, N. (2014). Mountaintop Removal Mining and Catchment Hydrology. *Water*, *6*(3), 472–499. https://doi.org/10.3390/w6030472

Moncrieff, J. B., Massheder, J. M., De Bruin, H., Elbers, J., Friborg, T., Heusinkveld, B., … Verhoef, A. (1997). A system to measure surface fluxes of momentum, sensible heat, water vapour and carbon dioxide.

Journal of Hydrology, *188–189*(1–4). https://doi.org/10.1016/S0022-1694(96)03194-0

Moncrieff, J., Clement, R., Finnigan, J., & Meyers, T. (2004). Averaging, detrending, and filtering of eddy covariance time series, in Handbook of micrometeorology. In *Handbook of Micrometeorology: A Guide for surface flux measurement and analysis*.

Murphy, J. C., Hornberger, G. M., & Liddle, R. G. (2014). Concentration-discharge relationships in the coal mined region of the New River basin and Indian Fork sub-basin, Tennessee, USA. *Hydrological Processes*, *28*(3). https://doi.org/10.1002/hyp.9603

Murray, C. D., & Buttle, J. M. (2003). Impacts of clearcut harvesting on snow accumulation and melt in a northern hardwood forest. *Journal of Hydrology*, *271*(1–4). https://doi.org/10.1016/S0022-1694(02)000352-9

Muscatello, J. R., & Janz, D. M. (2009). Selenium accumulation in aquatic biota downstream of a uranium mining and milling operation. *Science of the Total Environment*, *407*(4). https://doi.org/10.1016/j.scitotenv.2008.10.046

Myers, T. (2013). Remediation scenarios for selenium contamination, Blackfoot watershed, southeast Idaho, USA. *Hydrogeology Journal*, *21*(3). https://doi.org/10.1007/s10040-013-0953-8

Ni, W., Li, X., Woodcock, C. E., Roujean, J. L., & Davis, R. E. (1997). Transmission of solar radiation in boreal conifer forests: Measurements and models. *Journal of Geophysical Research Atmospheres*, *102*(24). https://doi.org/10.1029/97jd00198

Nicholls, E. M., Drewitt, G. B., Fraser, S., & Carey, S. K. (2019). The influence of vegetation cover on evapotranspiration atop waste rock piles, Elk Valley, British Columbia. *Hydrological Processes*, *33*(20), 2594–2606. https://doi.org/10.1002/hyp.13542

Nordstrom, D. K. (2011). Mine waters: Acidic to circumneutral. *Elements*, *7*(6). https://doi.org/10.2113/gselements.7.6.393

O'Kane Consultants Ltd. (2013). *Teck Coal watershed research and develpement program-record of soil moisture and meteorological performance monitoringsystem installation report.* Calgary.

Oke, T. R. (1987). *Boundary layer climates, Second edition*. *Inc.*

Palmer, M. A., Bernhardt, E. S., Schlesinger, W. H., Eshleman, K. N., Foufoula-Georgiou, E., Hendryx, M. S., … Wilcock, P. R. (2010). Mountaintop Mining Consequences. *Science*, *327*(5962), 148–149.

Pomeroy, J. W., & Granger, R. J. (1997). Sustainability of the western Canadian boreal forest under changing hydrological conditions. I. Snow accumulation and ablation. *IAHS-AISH Publication*, *240*.

Pomeroy, J. W., Gray, D. M., Hedstrom, N. R., & Janowicz, J. R. (2002). Prediction of seasonal snow accumulation in cold climate forests.

Hydrological Processes, *16*(18), 3543–3558. https://doi.org/10.1002/hyp.1228

Pomeroy, J.W., Gray, D. M., Brown, T., Hedstrom, N. R., Quinton, W. L., Granger, R. J., & Carey, S. K. (2007). The cold regions hydrological model: a platform for basing process representation and model structure on physical evidence. *Hydrological …*, *2667*, 2650–2667. https://doi.org/10.1002/hyp

Pomeroy, John, Fang, X., & Ellis, C. (2012). Sensitivity of snowmelt hydrology in Marmot Creek, Alberta, to forest cover disturbance. *Hydrological Processes*, *26*(12), 1891–1904. https://doi.org/10.1002/hyp.9248

Pomeroy, John W., & Gray, D. M. (1995). *Snowcover accumulation, relocation and management*. Saskatoon, Saskatchewan.

Pomeroy, JW, & Goodison, B. (1997). Winter and snow. *The Surface Climates of Canada*. Retrieved from http://books.google.com/books?hl=en&lr=&id=oxNMhw-rRrQC&oi=fnd&pg=PA68&dq=Winter+and+Snow&ots=SYZ_YjXvsy&sig=UfkYHV-HT1o-ix_Lr5g7FbO09tQ

Pomeroy, JW, & Granger, R. (2005). The process hydrology approach to improving prediction of ungauged basins in Canada. *Prediction in Ungauged …*, 67–100. Retrieved from http://www.usask.ca/hydrology/papers/Pomeroy_et_al_2004_2.pdf

Pomeroy, JW, Gray, D., & Shook, K. (1998). An evaluation of snow accumulation and ablation processes for land surface modelling. *… Processes*, *2367*(September), 2339–2367. Retrieved from http://onlinelibrary.wiley.com/doi/10.1002/(SICI)1099-1085(199812)12:15%253C2339::AID-HYP800%253E3.0.CO;2-L/abstract

Pomeroy, JW, & Parviainen, J. (1998). Coupled modelling of forest snow interception and sublimation. *Hydrological …*, *2337*(September), 2317–2337. Retrieved from http://onlinelibrary.wiley.com/doi/10.1002/(SICI)1099-1085(199812)12:15%253C2317::AID-HYP799%253E3.0.CO;2-X/abstract

Pomeroy, JW, & Schmidt, R. (1993). The use of fractal geometry in modeling intercepted snow accumulation and sublimation. *… of the Eastern Snow …*. Retrieved from http://www.westernsnowconference.org/sites/westernsnowconference.org/PDFs/1993Pomeroy.pdf

Pond, G. J., Passmore, M. E., Borsuk, F. A., Reynolds, L., & Rose, C. J. (2008). Downstream effects of mountaintop coal mining: Comparing biological conditions using family- and genus-level macroinvertebrate bioassessment tools. *Journal of the North American Benthological Society*, *27*(3). https://doi.org/10.1899/08-015.1

Rutter, N., Essery, R., Pomeroy, J., Altimir, N., Andreadis, K., Baker, I., … Yamazaki, T. (2009). Evaluation of forest snow processes models (SnowMIP2). *Journal of Geophysical Research Atmospheres*, *114*(6). https://doi.org/10.1029/2008JD011063

Schmidt, R. A., Jairell, R., & Pomeroy, J. W. (1988). Measuring snow interception and loss from an artificial conifer. *Proceedings 56 Th Western Snow Conference*.

Shatilla, N. J. (2013). *The Impact of Surface Mining on Runoff Timing and Flow Pathways, Elk Valley, British Columbia, Canada*. McMaster University.

Spittlehouse, D.L., Winkler, R. D. (1996). Forest canopy effects on sample size requirements in snow accumulation and melt comparisons. In *64 th. Western Snow Conference* (pp. 39–46). Bend, Oreg.

Spittlehouse, D. ., & Winkler, R. D. (2005). Snowmelt in a Forest and Clearcut. *Hyrdological Processes*, *19*.

SRK Consulting Ltd. (2010). *Selenium Geochemistry and Water Quality Predictions Phase 3 - Implementation 2009 Status Report DRAFT*.

Swanson, S. (2011). Presented by: Stella Swanson. In *Building stakeholder engagement in sustainable solutions: the strategic advisory panel on selenium management.*

Teck Resources Limited. (2014). *Teck 2014 Annual Report*. Vancouver. Retrieved from http://www.teck.com/media/Investors-teck_2014annualreport_T5.1.1.pdf

Teck Resources Limited. (2021). Steelmaking Coal.

Toews, D., & Gluns, D. (1986). Snow Accumulation and Ablation on Adjacent Forested and Clearcut Sites in Southeastern British Columbia. In *Western Snow Conference, April 15-17, 1986, Phoenix Arizona*.

USACE. (1998). *Engineering and Design. Runoff From Snowmelt*. *Engineer Manual*.

Vickers, D., & Mahrt, L. (1997). Quality control and flux sampling problems for tower and aircraft data. *Journal of Atmospheric and Oceanic Technology*, *14*, 512–526.

Villeneuve, S. A., Barbour, S. L., Hendry, M. J., & Carey, S. K. (2017). Estimates of water and solute release from a coal waste rock dump in the Elk Valley, British Columbia, Canada. *Science of the Total Environment*, *601–602*, 543–555. https://doi.org/10.1016/j.scitotenv.2017.05.040

Watson, F. G. R., Anderson, T. N., Newman, W. B., Alexander, S. E., & Garrott, R. a. (2006). Optimal sampling schemes for estimating mean snow water equivalents in stratified heterogeneous landscapes. *Journal of Hydrology*, *328*(3–4), 432–452. https://doi.org/10.1016/j.jhydrol.2005.12.032

Wayland, M., & Crosley, R. (2006). Selenium and other trace elements in aquatic insects in coal mine-affected streams in the Rocky Mountains of Alberta, Canada. *Archives of Environmental Contamination and Toxicology*, *50*(4), 511–522. https://doi.org/10.1007/s00244-005-0114-

8
Webb, E.K., Pearman, G.I., Leuning, R. (1980). Correction of flux measurements for density effects due to heat and water vapour transfer. *Quarterly Jounrnal of the Royal Meteorological Society*, *106*(447), 85–100.
Wellen, C., Shatilla, N. J., & Carey, S. K. (2015). Regional scale selenium loading associated with surface coal mining, Elk Valley, British Columbia, Canada. *Science of the Total Environment*, *532*, 791–802. https://doi.org/10.1016/j.scitotenv.2015.06.040
Wellen, C., Shatilla, N. J., & Carey, S. K. (2018). The influence of mining on hydrology and solute transport in the Elk Valley, British Columbia, Canada. *Environmental Research Letters*, *13*(7). https://doi.org/10.1088/1748-9326/aaca9d
Wilczak, J.M., Oncley, S.P. & Stage, S. A. (2001). Sonic Anemometer Tilt Correction Algorithms. *Boundary-Layer Meteorology*, *99*, 127–150.
Winkler, R., & Boon, S. (2014). Snow accumulation and ablation response to changes in forest structure and snow surface albedo after attack by mountain pine beetle. *Hydrological …*. https://doi.org/10.1002/hyp
Woo, M. K. (1997). A Guide for Ground Based Measurement of the Arctic Snow Cover. *Atmospheric Environment*, (December).
World Coal Association. (2015). World Coal Assocation. Retrieved December 20, 2015, from https://www.worldcoal.org
Younger, P. L. (2004). Environmental impacts of coal mining and associated wastes: A geochemical perspective. *Geological Society Special Publication*. https://doi.org/10.1144/GSL.SP.2004.236.01.12